PG
Petroleum Geoscience

Research article

https://doi.org/10.1144/petgeo2020-123 | Vol. 27 | 2021 | petgeo2020-123

Identification and characterization of geological formations with CO_2 storage potential in Portugal

Pedro Pereira[1*], Carlos Ribeiro[1,2,3] and Júlio Carneiro[1,2]

[1] Instituto de Ciências da Terra, Escola de Ciências e Tecnologia, Universidade de Évora, Rua Romão Ramalho 59, 7000-671 Évora, Portugal
[2] Departamento de Geociências, Escola de Ciências e Tecnologia, Universidade de Évora, Rua Romão Ramalho 59, 7000-671 Évora, Portugal
[3] MARE – Centro de Ciências do Mar e do Ambiente, Universidade de Lisboa, Campo Grande 016, 1600-548 Lisboa, Portugal
PP, 0000-0001-6156-8044
* Correspondence: pmpereira@uevora.pt

Abstract: Carbon capture, utilization and storage (CCUS) is considered a major part of the Portuguese strategy for reducing CO_2 emissions. Some industrial sectors, the most prominent being the cement sector, require the implementation of CO_2 storage to reach carbon neutrality by 2050. This paper presents and characterizes the areas with potential for CO_2 storage in mainland Portugal. The lithostratigraphic and tectonic frameworks of the onshore and offshore basins are presented; a site screening process was conducted, based on basin- and regional-scale assessments, resulting in the definition of eight possible storage clusters, seven of which are offshore. The storage capacity was estimated for those clusters, with a central (P_{50}) value of 7.09 Gt; however, the most interesting locations are in the Lusitanian Basin (West Iberian Margin), both onshore and offshore, as they present high capacity and are located favourably in relation to the industrial CO_2 emitters. Considering only the potential sites of this basin, their storage capacities are greater than 3 Gt CO_2, of which 260 Mt are onshore.

Thematic collection: This article is part of the Geoscience for CO_2 storage collection available at: https://www.lyellcollection.org/cc/geoscience-for-co2-storage

Received 3 November 2020; **revised** 22 January 2021; **accepted** 29 January 2021

Context for CCUS in the energy and industry policies in Portugal

The solution to solve global warming is non-linear and non-unique but the importance of CO_2 capture, utilization and storage (CCUS) technologies has been identified and accepted as part of the solution for climate change mitigation at the European Union (EU) and global level. This vision has further been stressed by the Paris Climate Agreement (UNFCCC 2015). The scenarios developed by the International Energy Agency (IEA: IEA 2017) demonstrate that by 2060, CCUS should contribute to 14% of the required reduction in CO_2 emissions to achieve a scenario where the global temperature increase by 2100 is less than 2°C, or 32% of the reduction to achieve the 1.5°C limit scenario.

Portugal's commitment to achieve carbon neutrality by 2050 has resulted in a national roadmap, Roadmap for Carbon Neutrality 2050 (RNC2050: APA 2019), that identifies and analyses the alternative trajectories that are technically feasible, economically viable and socially accepted to achieve a carbon neutral economy by 2050. The RNC2050 does not foresee any significant role for CCUS in the path of the national energy system to carbon neutrality.

However, the rapid decrease in the costs of renewable energy production encouraged the Portuguese authorities to envisage an energy system in which green hydrogen (i.e. produced from renewable energy sources) plays an important role. The National Strategy for Hydrogen (EN-H_2) (DGEG 2020) forecasts that, from 2025 onwards, carbon capture and utilization (CCU) will be an essential component to convert the green hydrogen into methane and aviation kerosene. The anticipated demand of CO_2 capture for that purpose is approximately 1 metric ton per year (Mt a^{-1}) in 2030 (DGEG 2020). Hence, CCU is now seen as essential for the new energy strategy in the country.

Furthermore, and although Portugal lacks a significant heavy industry, the industry sector represents approximately 17% of the total CO_2 emissions, comprising *c.* 8 Mt a^{-1} (IEA 2018). According to Seixas *et al.* (2015), the cement sector is the industry that will most likely require CO_2 storage, due to its high process emissions. Roughly two-thirds of the *c.* 4 Mt a^{-1} of CO_2 emitted by the sector in 2018 (EU-ETS 2018) are related to industrial processes and cannot be mitigated through fuel switch. Carbon neutrality in those industrial sectors with high process emissions will require geological storage of CO_2.

The role for CO_2 storage is further enhanced by the possibility of achieving negative emissions through bioenergy with carbon capture and storage (BECCS) deployment in the paper and pulp sector, which was responsible for CO_2 emissions of 5.40 Mt a^{-1} in 2017 (E-PRTR 2017), most of which resulted from biomass being used as the main fuel. Therefore, CO_2 storage must be an integral component of the convergence to carbon neutrality in the industrial sector of the country.

Figure 1a shows the geographical distribution of CO_2 emission point sources in mainland Portugal in 2018 (EU-ETS 2018). Power and refinery activities were responsible for *c.* 11.3 and 3.2 Mt a^{-1} of CO_2 emissions, respectively. The two largest sources in the country, the Sines and Pego coal power plants, which accounted for 39% of total CO_2 emissions from stationary sources in 2018, and a refinery in Porto, will be decommissioned until 2023, significantly reducing the national emissions. However, stationary facilities from the industrial sector will remain as relevant sources, in particular the six cement plants, which have a significant impact on the Portuguese emissions budget. In addition to the cement, and pulp and paper

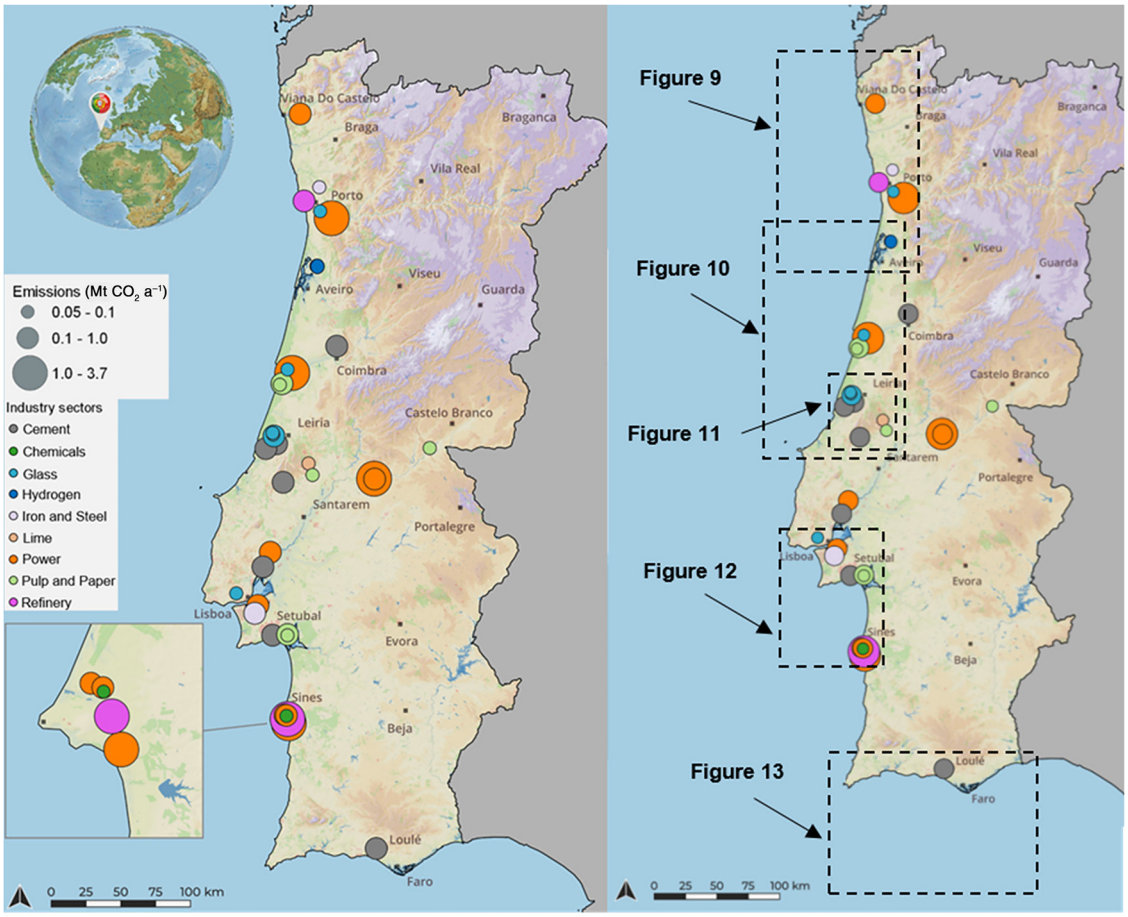

Fig. 1. (**a**) Geographical distribution of main CO_2 emission sources by industrial sectors in Portugal. Only sources with emissions above 50 kt a^{-1} are represented. Data are from EU-ETS (2018). Sources in the inset detailing the Sines industrial area are slightly displaced to avoid overlap and show the diversity of industries in the area. (**b**) Location of study areas for CO_2 storage addressed hereafter and the geographical distribution of the main CO_2 sources.

industries, other industrial activities such as glass (0.62 Mt a^{-1}), and iron and steel (0.14 Mt a^{-1}) also present important CO_2 emissions that should not be neglected. The main CO_2 sources are located along or near the coastline of the country, which generally are close to the study areas with potential for CO_2 storage presented hereafter (Fig. 1b).

Several geological environments for CO_2 storage were studied in recent years by Portuguese research teams: coal seams (Lemos de Sousa *et al.* 2007), mineral carbonation in ultramafic and mafic rocks (Romão *et al.* 2016; Moita *et al.* 2020), CO_2 hydrates in subseabed sediments (Bernardes *et al.* 2013, 2015) and deep saline aquifers (e.g. Carneiro *et al.* 2011). The option for CO_2 storage in deep saline aquifers (DSA) remains the most promising in the Portuguese geological context and is the subject of this paper.

This paper summarizes studies conducted in Portugal in the scope of the FP7 COMET project, and the nationally funded KTEJO and CCS-PT projects, to identify DSA national resources for CO_2 geological storage, and ultimately to assess the feasibility of applying CCUS technology in Portugal in its geological storage component. First an overview of the lithostratigraphic and tectonic frameworks of the sedimentary basins is presented. Then the several methods applied and the dataset available to conduct this work are described. The results of this work encompass the identification and characterization of suitable geological formations for CO_2 storage, the estimation of storage capacity, and a discussion about source–storage site match, while accounting for the clustering of storage units in each of the studied sedimentary basins.

Lithostratigraphic and tectonic frameworks of sedimentary basins

The West and SW Iberian margins evolved through a sequence of rift episodes from the Late Triassic to the Early Cretaceous during the synrift, post-rift and passive-margin phases of the North Atlantic evolution (Terrinha *et al.* 2019*b*). Overlying the Paleozoic and Proterozoic basement are sedimentary Mesozoic and Cenozoic basins, bordering the Portuguese Atlantic margin, which are potential targets for CO_2 storage (Fig. 2a). The structure of these basins is strongly controlled by prominent Variscan lineaments, inherited from a late phase (Permian) of strike-slip deformation (Ribeiro *et al.* 1979; Pinheiro *et al.* 1996). These include the NNE–SSW and NNW–SSE to NW–SE listric and/or planar normal faults, and NE–SW to ENE–WSW transverse faults, delimiting the main depositional systems identified along the margin (Wilson *et al.* 1989; Murillas *et al.* 1990; Pinheiro *et al.* 1996; Capdevila and Mougenot 1998; Alves *et al.* 2006). During the Alpine compression, from the Late Cretaceous onwards, some of the faults were reactivated as reverse or thrust faults, sometimes with a strike-slip component (Boillot *et al.* 1979; Mauffret *et al.* 1989; Masson *et al.* 1994).

The site screening for CO_2 storage focused on the following sedimentary basins (Fig. 2a):

- The Meso-Cenozoic basins on the Western Iberian Margin, including the Lusitanian Basin (onshore and offshore) and the Porto Basin (offshore). For the purpose of this work, the

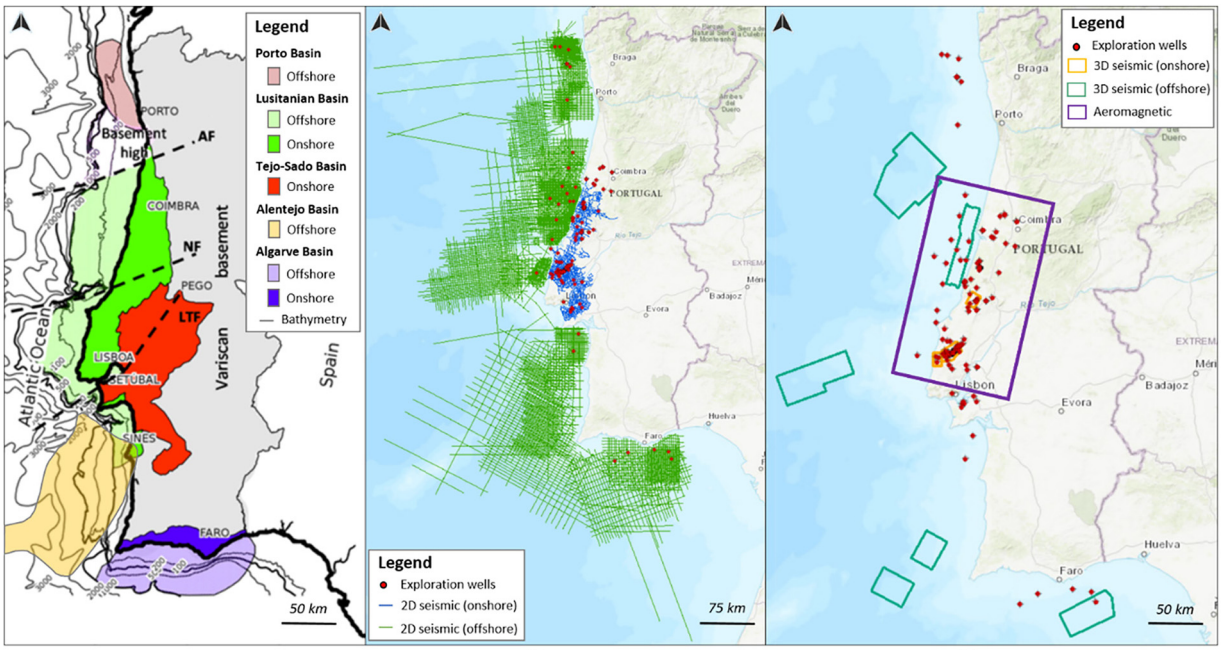

Fig. 2. (**a**) Sedimentary basins in Portugal (both onshore and offshore settings) and some major faults. (**b**) Database (DGEG 2020) illustrating the geographical distribution of the 2D seismic surveys. (**c**) 3D seismic and the aeromagnetic surveys and legacy exploration wells available for the site screening in Portugal.

Lusitanian Basin designation refers to study areas located in the northern and central sectors of this basin, while the screening assessment conducted in the southern sector of the Lusitanian Basin is hereafter designated as the Alentejo Basin. In fact, the limits of this sector virtually coincide with the beginning of the shallow offshore coverage of the Alentejo Basin (Fig. 2a);

- the Meso-Cenozoic Algarve Basin (onshore and offshore), along the south margin of the Portuguese territory; and
- the Cenozoic Tagus-Sado Basin (onshore).

The Porto, Lusitanian and Algarve basins constitute most of the Portuguese continental shelf, with a larger volume of sedimentary rocks than the volume outcropping onshore. The physiographical characteristics of the Portuguese continental shelf, and the areal extent and thickness of the Mesozoic and Cenozoic formations, have raised most interest in the offshore sector as a target for CO_2 storage screening opportunities (Carneiro *et al.* 2011).

The following subsections provide detailed descriptions of the lithostratigraphic and tectonic frameworks of the Meso-Cenozoic sedimentary basins (including the Alentejo Basin). A detailed description of the entirely onshore Cenozoic Tagus-Sado Basin is not included in this work because the basin-scale assessment criteria adopted in the COMET project (Martinez *et al.* 2010) indicates that the basic requirements are not met for CO_2 storage. Nonetheless, a brief explanation about the main obstacles of this basin is addressed in the beginning of the Results section.

Porto Basin

The Porto Basin narrows (*c.* 50 km wide) and extends between the coast and the outer continental shelf, and is slope bounded to the north by the Galicia Interior Basin, to the south by the Aveiro horst and to the west by the Peniche Basin (Pinheiro *et al.* 1996). The shallow offshore portion of the basin comprises a *c.* 4 km-thick sedimentary sequence spanning the Late Triassic–Late Cretaceous (Moita *et al.* 1996) (Fig. 3). The basin is in the northward continuation of the Lusitanian Basin, delimited to the east by the Porto-Tomar Fault (Fig. 2a), a major late Variscan lineament that was active throughout most of the basin evolution (Alves *et al.* 2006; Cunha 2008). The stratigraphy of Porto Basin is based on data from previous hydrocarbon exploration wells and from the

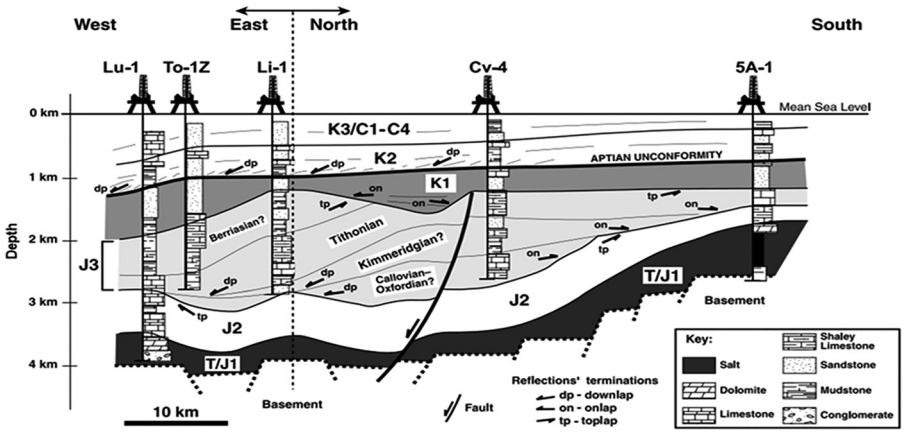

Fig. 3. Interpreted seismic section from the shallower Porto Basin (adapted from Alves *et al.* 2006). Seismic units (from bottom to top): T-J1, Triassic; J2, Sinemurian, Lower Jurassic; J3, Jurassic; K1, Berriasian–Early Valanginian; K2, Late Aptian–Albian; K3/C1–C4, Turonian–Middle Pliocene. See Figure 9b for the location of the seismic section. AAPG ©2006, reprinted by permission of the AAPG whose permission is required for further use.

Table 1. *Chronostratigraphic description of geological formations in the Porto Basin*

Chronostratigraphy	Formation	Lithology
Paleogene	Espadarte Formation	Dolomite, alternation of clay and fine–coarse sandstone are present (Witt 1977) deposited in a fluvial/lacustrine to restricted marine environment (Cunha 2008)
Upper Campanian–Maastrichtian	Dourada Formation	Dolomite-cemented quartz arenites grading to sandy crystalline dolostones with intercalations of marls (Witt 1977) deposited in fluvial to very-shallow-marine environments (Dinis *et al.* 2008)
Coniacian–Upper Campanian	Carapau Formation	Silty–sandy argillaceous limestone and limestone with marl intercalations. In the lower half of the formation, additional intercalations of very-fine, calcareous-cemented quartz sandstone have been described (Witt 1977)
Upper Turonian	Gândara Formation	Sandstone grading to conglomerate, with intercalations of dolomite-cemented quartz sandstone and clay (Witt 1977)
Upper Cenomanien	Cacém Formation	Upper member is composed mainly of limestone (packstone/grainstone). Lower member is argillaceous, dolomitic, calcareous (mudstone/wackestone) grading to marly and argillaceous calcareous dolomite to dolomitic limestone (Witt 1977)
Lower Cretaceous–Middle Cenomanian	Torres Vedras Group	Coarse quartz sandstone, grading to conglomerate, with intercalations of fine-grained quartz sandstone grading into silty or sandy clay, marl and clay. At the base of the sequence there is a predominance of coarse-grained, conglomeratic quartz sandstone (Witt 1977)
Upper Jurassic–Tithonian	Linguado Formation	Composed, from top to bottom, of sandstone, marls and minor limestone deposited in shallow-marine to fluvial-deltaic environments
Lower–Middle Jurassic	Esturjão Formation	Sequence of alternating carbonates and shales (Alves *et al.* 2006). Argillaceous limestone and mudstone, grading to variegated marl and calcareous claystone, in places rich in anhydrite in the lower half of the sequence (Witt 1977). Equivalent to the Brenha and Candeeiros formations in the Lusitanian Basin
Upper Triassic–Hettangian	Dagorda Formation	Mainly composed of rock salt, interbedded with occasional clays, limestones, mudstones and anhydrite. Dark grey to black shale streaks within the Dagorda evaporite sequence occur in the centre of the salt province (Witt 1977)
Upper Triassic	Silves Group	Red fluvial sandstones and siltstones, sandy-conglomeratic. Towards the basin centre the grain size of the Silves sandstones progressively diminish. The upper part of the sequence consists of shale, overlain by Dagorda Formation evaporites (Witt 1977)

interpretation of seismic profiles (Witt 1977; Moita *et al.* 1996; Alves *et al.* 2006). Moreover, this stratigraphy is correlated with the stratigraphy established for the Lusitanian Basin, where well data are more abundant and the formations are also exposed onshore (Witt 1977; Wilson 1988). The main lithostratigraphic units of this basin are presented in Table 1.

Lusitanian Basin

The Lusitanian Basin extends along the West Iberian Margin, trending NNE–SSW, and covers *c.* 20 000 km^2 in the west-central part of mainland Portugal and the adjacent continental shelf. In fact, this basin is defined as the area between the coastal town of Aveiro in the north and the coastal area south of the Arrábida Chain (Wilson *et al.* 1989; Rasmussen *et al.* 1998). The western limit of the basin is bound by the 'slope fault system' (Alves *et al.* 2006) and, in places, by prominent horsts (e.g. the Berlengas Horst), and the eastern limit is bound by the Porto-Tomar Fault (Fig. 2a), which delimits the Hercynian Massif (Ribeiro *et al.* 1979; Wilson *et al.* 1989; Pinheiro *et al.* 1996).

The formation of this basin occurred over a sequence of rift pulses between the Late Triassic and the Early Cretaceous (Wilson *et al.* 1989; Pinheiro *et al.* 1996; Rasmussen *et al.* 1998; Alves *et al.* 2002; Alves *et al.* 2009). The first rift phase (Late Triassic) occurred within normal fault-bound half-graben, interpreted by the variations in thickness and depositional facies (Alves *et al.* 2003); the onset of marine deposition, together with a relative increase in regional thermal subsidence, marks the second rift during the Sinemurian–Pliensbachian (Rasmussen *et al.* 1998; Alves *et al.* 2003). The third rifting episode (Late Oxfordian–Kimmeridgian) resulted in relatively thick synrift sequences deposited in several sub-basin systems (Wilson 1988; Leinfelder and Wilson 1998; Rasmussen *et al.* 1998). During this rifting phase, two distinct depositional stages were recorded: (1) a period of widespread carbonate deposition in lacustrine to deep-marine environments; and (2) the influx of marine to fluvial siliciclastic sediments (Leinfelder and Wilson 1998; Alves *et al.* 2003).

Continental break-up and subsequent opening of the North Atlantic Ocean occurred during the Valanginian–Early Aptian and led to the deposition of a thick sequence of coarse-siliciclastic sediments (Alves and Cunha 2018). From the Aptian–Albian and onwards, a passive continental margin was established in western Iberia, with oceanic accretion to the west (Pinheiro *et al.* 1996). During the Late Cretaceous–Late Miocene, important changes associated with the collision of the Iberia microplate with Eurasia or Africa led to the reactivation of extensional faults developed during the rifting stages (Fig. 4) (Terrinha *et al.* 2019*a*).

The Lusitanian Basin has an extensive onshore area (Fig. 2a) in which the Mesozoic sedimentary formations crop out. Based on the facies variations and the thicknesses of the lithostratigraphic units, the Lusitanian Basin can be divided into three sectors bounded by major faults (Rocha and Soares 1984; Pinheiro *et al.* 1996; Alves *et al.* 2006):

- The Northern sector, bound by the Aveiro Fault to the north and the Nazaré Fault to the south (Fig. 2a), where the Early–Middle Jurassic and Cretaceous–Paleogene sequences are well preserved;
- the Central sector, defined between the Nazaré Fault in the north, and the Montejunto-Arrife Fault (onshore) and the Estremadura Spur (offshore) to the south. The Middle Jurassic outcrops are well preserved, with substantial thickness, contrary to the Late Jurassic and part of the Cretaceous, which have been largely eroded; and
- the Southern sector, where the Late Triassic–Late Jurassic and part of the Tertiary sections are well preserved.

A lithostratigraphic description of the main geological units from the offshore area is presented in Table 2. The lithostratigraphic sequence in the sedimentary basin shows no major differences to the offshore sequence.

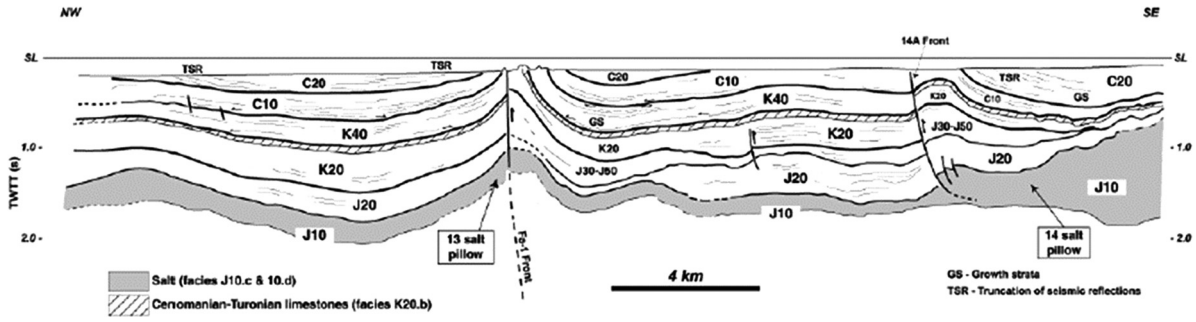

Fig. 4. Interpreted section of seismic line S84-26 from the Lusitanian Basin (adapted from Alves *et al.* 2003). Seismic units (from bottom to top): J10, Triassic; J20, Lower Jurassic; J30–J50, Oxfordian–Barremian; K20, Aptian–Turonian; K40, Campanian–Maastrichian; C10, Paleocene–Eocene; C20, Late Oligocene–Plio-Pleistocene. See Figure 10a for the location of the seismic section. SL, sea level.

Alentejo Basin

The Alentejo Basin is the southern rift basin of the West Iberian Margin (Fig. 2a) and is separated from the Lusitanian Basin by the Arrábida Chain, which is a fold and thrust belt formed during the tectonic Miocene shortening event. The study area is located in the shallow offshore area of this basin and has a western limit defined by the 200 m bathymetric line.

The study area shares structural aspects with the West Iberian Margin, as a Mesozoic non-volcanic rift margin that evolved through several rift pulses interspersed with periods of tectonic quiescence between the Late Triassic and the Late Cretaceous (Wilson *et al.* 1989; Rasmussen *et al.* 1998; Alves *et al.* 2006, 2009) (Fig. 5).

The structure of the basin is strongly controlled by prominent late Variscan lineaments (Late Carboniferous–Early Permian: Ribeiro *et al.* 1979; Pinheiro *et al.* 1996). This includes NNE–SSW and NNW–SSE to NW–SE listric and/or planar normal faults, and NE–SW to ENE–WSW transverse faults (Fig. 5), delimiting the main depositional systems identified along the margin (Wilson *et al.* 1989; Capdevila and Mougenot 1998; Alves *et al.* 2006, 2009). Two geological profiles of Figure 5 illustrate the overall structure and geometry of the strata within the study area, highlighting: (a) pervasive sets of normal faults cutting through the Mesozoic and, in places, Cenozoic sequences; (b) relatively thin Mesozoic sequences, when compared with other areas along the West Iberian Margin; (c) almost uniform thickness of Late Triassic–Middle Jurassic sequence,

Table 2. *Chronostratigraphic description of geological formations in the Lusitanian Basin*

Chronostratigraphy	Formation	Lithology
Oligocene–Miocene and younger	Moreia Formation	Coarse sand grading to gravel. A white, sandy limestone bed has been described near the base (Witt 1977)
Oligocene	Benfica Formation	Variegated marl and clay, calcareous conglomerate, and a conglomerate underlain by limestone of varied compaction (GPEP 1986)
Paleogene	Espadarte Formation	Dolomite, alternation of clay and fine–coarse sandstone is present (Witt 1977) deposited in a fluvial/lacustrine to restricted marine environment (Cunha 2008)
Late Campanian–Maastrichtian	Dourada Formation	Dolomite-cemented quartz sandstone, grading to sandy, very-fine crystalline dolomite and, in the lower part, intercalations of marly and occasionally sandy limestone (GPEP 1986)
Turonian–Coniacian	Gândara Formation	Sandstone grading to conglomerate, with intercalations of dolomite-cemented quartz sandstone and clay (Witt 1977)
Cenomanian–Early Turonian	Cacém Formation	Mainly limestone deposited in a marine carbonate platform (Kullberg 2000)
Early Cretaceous–Cenomanian	Torres Vedras Group	Mainly sandstones, deposited in a fluvial environment (Kullberg 2000; Carvalho *et al.* 2005)
Kimmeridgian–Tithonian	Grés Superiores/Lourinhã Formation	Sandstones, sometimes with levels of conglomerates and marly limestones. This unit was deposited in a meandering fluvial system on an alluvial plain (Kullberg 2000)
Kimmeridgian	Alcobaça Formation	Alternating sandy and marly, detrital limestone deposited in a shallow carbonate–siliciclastic platform environment (Kullberg 2000)
Late Oxfordian	Montejunto Formation	Carbonate sequences with interbedded mudstones. The formation is characteristic of a shallow-marine environment of a carbonate platform system with episodical sedimentation of clay (Kullberg 2000)
Middle Oxfordian–Early Kimmeridgian	Cabo Mondego Formation	Marls, clay and marly limestones interbedded with bituminous, lignite and sandstone (Kullberg 2000; Azerêdo *et al.* 2003). The Cabo Mondego Formation is characteristic of coastal plain to restricted carbonate shelf depositional environment (Witt 1977)
Sinemurian–Callovian	Brenha Formation	Subdivided into two members: (1) the base: a succession of poorly fossiliferous dolomites and dolomitic limestones; and (2) the upper section: mainly limestones intercalated with centimetre-thick layers of marls (Azerêdo *et al.* 2003)
Late Triassic–Hettangian	Dagorda Formation	Subdivided into three members (Witt 1977; Carvalho *et al.* 2005): (1) a lowermost section, with dominant halite and possible stringers of dolomitic shales and anhydrite; (2) an intermediate salt/dolomite member; and (3) an uppermost section composed of dolomite and anhydrite beds. Deposited in an alluvial plain setting, with episodic marine incursions, and where a rapid subsidence was followed by the deposition of a thick column of evaporites (Kullberg 2000)
Upper Triassic	Silves Group	Siliciclastic deposits, sandy and sandy-conglomeratic at the base, and pelitic with dolomite intercalations at the top. The siliciclastic member accumulated in an alluvial-fan environment, under fault-controlled subsidence (Rasmussen *et al.* 1998). This formation occupied channels of the residual relief of the Hesperian massif and faulted, tilted blocks, producing the variable thicknesses encountered in several wells along the Lusitanian Basin (Carvalho *et al.* 2005)

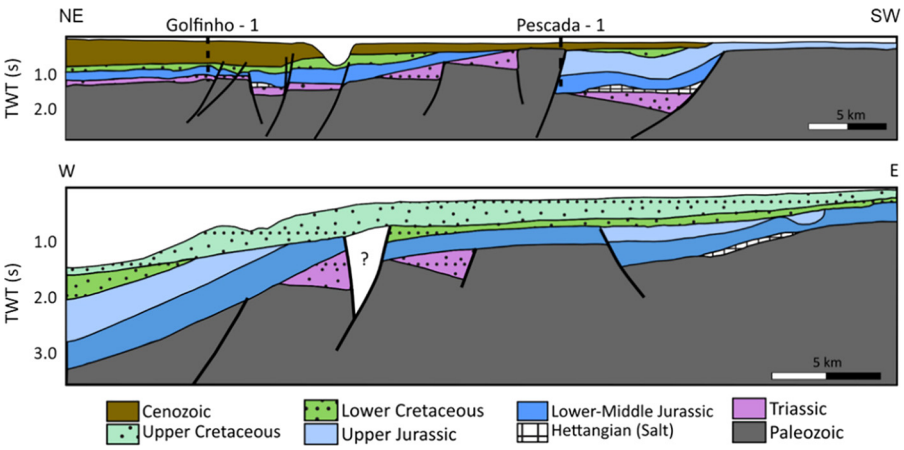

Fig. 5. NE–SW and west–east cross-sections illustrating the geological structures and fault systems of the Alentejo Basin. See Figure 12 for the location of the geological profiles.

corresponding mostly to carbonate ramp deposition (Alves *et al.* 2009); and (d) the absence of salt structures, which is consistent with the outcrop information from the study area (onshore), where the Triassic–Hettangian evaporites are absent (Alves *et al.* 2009).

The shallow offshore area of the Alentejo Basin encompasses the southernmost Lusitanian Basin. This sub-basin (as designated by some authors) is the least explored in the offshore area of Portugal, with only two petroleum exploration boreholes (Golfinho-1 and Pescada-1) drilled and with lower-quality seismic surveys. A summarized description of the main lithostratigraphic units in the study area, adapted from Inverno *et al.* (1993) and Pereira and Alves (2012), is presented in Table 3.

Algarve Basin

The offshore Algarve Basin (Fig. 2c) is located on the southwestern margin of the Iberian Peninsula, just north of the Azores–Gibraltar Fracture Zone, marking the present-day boundary between the Nubia and Eurasia tectonic plates (Ribeiro *et al.* 1979; Terrinha 1998; Lopes *et al.* 2006).

During the Mesozoic, the basin evolved as a rift basin (Terrinha 1998) in a transtensional tectonic setting because of the differential eastward movement of the African and Eurasian plates with the formation of Tethys Ocean. The crustal stretching was accommodated by the reactivation of late-Variscan NE–SW to east–west lithospheric faults that are frequently segmented by north–south to NW–SE faults (Terrinha 1998; Terrinha *et al.* 2002) and were reactivated both during Mesozoic rifting and during Late Cretaceous–recent compressional events (Terrinha 1998; Zitellini *et al.* 1999; Dias 2001; Terrinha *et al.* 2003; Ramos *et al.* 2020). The Cenozoic basin is a flexural-type basin, associated with the Alpine orogenic event and compressive stresses from the Mid-Miocene onwards (Terrinha 1998).

Thus, Algarve Basin sediments record two superimposed depositional cycles: (1) the Mesozoic rift basin (Triassic–Early

Table 3. *Chronostratigraphic description of geological formations in the Alentejo Basin*

Chronostratigraphy	Formation	Lithology
Miocene–Pliocene	—	Medium- to coarse-grained sandstones interbedded with siltstones and shales deposited in a shallow-marine environment. The onshore counterpart is mainly calciclastic sandstones, fine-grained sandstones and gravely sandstones
Mid-Aptian–Maastrichtian/ Paleocene	—	Absent onshore and frequently absent boreholes, this time interval is characterized by siliciclastic sediments deposited as deltaic wedge or prograding slope deposits
Berriasian–Mid-Aptian	—	Absent onshore, Cretaceous sedimentation started during the Berriasian after a Tithonian–Berriasian disconformity. The older sediments are shallow-marine siliciclastics that are overlain by deep marine carbonates
Oxfordian–Kimmeridgian	Deixa-o-Resto Formation	Starts with a thick unit of polygenic conglomerates with marls intercalations, overlain by calciclastic limestones and oolithic limestones interlayered with marls and clays
Bathonian–Callovian	Rodeado Formation (Bathonian) and Monte Branco Formation (Callovian)	Calciclastic limestones, sometimes oolithic limestones and minor dolomites; strong karstification affect this formation. The Monte Branco Formation is essentially formed by calciclastic limestone with rare micritic limestones and microconglomerates. Towards the top of the formation, quartz and feldspar clasts increase their abundance
Sinemurian–Toarcian	Fateota Formation	Dolomites, dolomitic marls and limestones are the main constituents onshore. Towards the north, the siliciclastic sediments predominate. Offshore, in the deeper part of the basin, dolomites also predominate along with pelites
Hettagian–	Volcano-sedimentary complex	Deposits of holeiitic basalts alternating with dolomitic marls and limestone (onshore). Towards the deeper part of the basin (offshore) no volcanic rocks were described, and the deposits of this age are essentially dolomites and dolomitic limestones deposited in a shallow-marine environment
Rhaetian–Hettangian	Silves pelitic-carbonate evaporite Complex (Dagorda Formation?)	Continental margin deposits evolving to restricted marine conditions. The sediments are mainly shales, evaporites and limestones; towards the top, dolomitic sediments predominate with silt and clay intercalations
Upper Triassic	Silves Group	Siliciclastic deposits of alluvial-fan systems, mainly red sandstones with conglomeratic and pelitic intercalations. The matrix consists of clay and iron oxides. Given the fact that the sedimentation of this unit was controlled by the geometry of small basins in the Hesperic massif, its thickness is variable, even in deep offshore areas of the basin

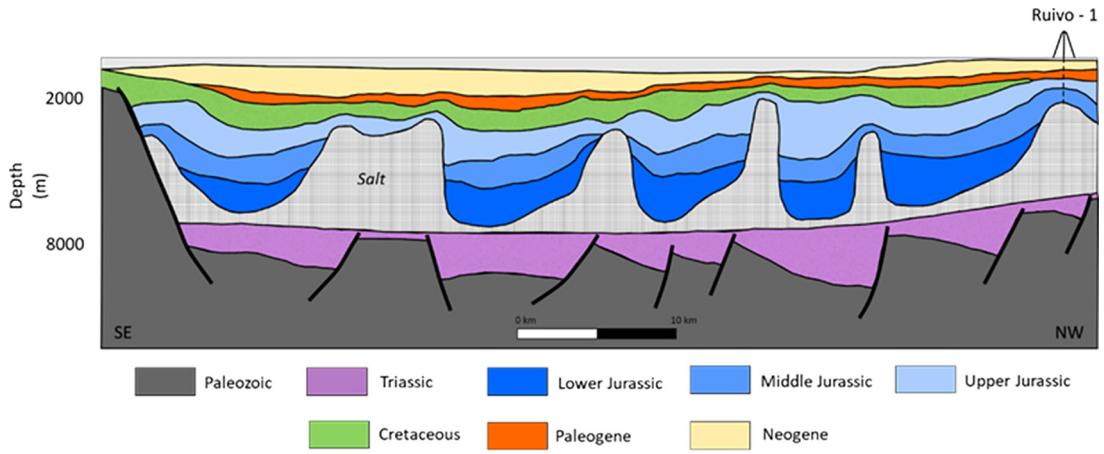

Fig. 6. Schematic cross-section (2D depth model) illustrating the major structures identified in the offshore portion of the Algarve Basin (adapted from Matias 2007). See Figure 13 for the aerial location of the geological cross-section.

Cretaceous); and (2) the Cenozoic compressional basin (Late Cretaceous onwards). Both cycles are separated by the Turonian–Burdigalian hiatus, corresponding to the main phase of tectonic inversion and uplift (Terrinha 1998). The presence of large evaporite complexes (Fig. 6), deposited during the Triassic–Hettangian transition, influenced the tectonic style of the younger sedimentary cover, acting as a detachment during both extension and compression events (Lopes *et al.* 2006). The Algarve Basin has

Table 4. *Chronostratigraphic description of geological formations in the Algarve Basin*

Chronostratigraphy	Lithology
Plio-Quaternary	Variety of lithologies including clays sands and gravels. In its western section, the Algarve Basin consists mainly of claystones, the central part is mostly sands, and the eastern sector is dominated by clay with minor intercalation of sand and siltstones (Matias 2007)
Late Miocene	Basal section of conglomerates (Tortonian) overlain by silt and biocalcarenites, while the Messinian is characterized mainly by fluvial sand deposits (Roque 2007)
Middle Miocene	Variety of lithologies such as limestone, sand, clay and siltstone (Matias 2007)
Early Miocene	Limestones in the west, interbedded sandstones and siltstones in the central part of the basin, overlain by limestones with some corals, and highly fractured limestone and marls towards the east (Matias 2007)
Oligocene	Dominated by micritic limestones and skeletal limestones with minor dolomites and clays
Eocene	Mainly characterized by limestones, dolomitic in parts
Paleocene	Sands, sandstones and marls
Late Cretaceous	The absence of this unit in most of wells from the Algarve's offshore suggests the presence of an important, regional erosion unconformity or depositional hiatus (Matias 2007)
Early Cretaceous	Onshore, the western and central sectors include marls, sandstones, limestones and dolomites, while the eastern sector is characterized by predominantly limestones and marls with some less abundant dolomites. The Upper Barremian is a sequence of sandstones and clays (Terrinha *et al.* 2006). Offshore, in the western sector, the Berriasian–Hauterivian recovered in the Imperador-1 well consists of a basal layer of sand, followed by an interbedded sequence of shales and limestones, overlain by dolomites and claystone. In the central area, the Corvina-1 well recovered sandy layers at the Berriasian, overlain by a sequence of shaly silt and dolomites, grading into marls with some beds of limestones in the top. Lastly, in the eastern sector (Algarve-1 well), the Berriasian–Hauterivian consists of grey argillaceous sandstones with minor shales and clays. The Aptian–Albian sequence in the western sector consists of a sequence of shales and limestones, interbedded with claystones and minor layers of sands at the top (Imperador-1 well). The central area (Corvina-1 well) is characterized by oolitic limestone at the base of the sequence, and by interbedded sand silt with some layers of limestone at the top. To the east, the Algarve-1 well recovered a sequence of interbedded argillaceous sandstones, claystones and siltstones, with micritic limestones towards the top of the section (Matias 2007)
Late Jurassic	Onshore, at the western sector of the basin, the sediments are mainly limestones, sometimes with phosphate nodules, marly limestones and dolomitic limestones, while in the (thicker) eastern sector limestones, sometimes with chert nodules, marly limestones and dolomitic limestones are the most common lithologies. Offshore, in the western sector of the Algarve Basin (Imperador-1 and Ruivo-1 wells), the Late Jurassic consists mainly of a massive, light limestone, with thin, interbedded claystone and shaly limestone layers, overlain by siltstones, whilst in the east (Algarve-1 well) it is predominantly interbedded siltstones, shales and marls with very minor sandstones. Therefore, the Late Jurassic shows a lateral change from carbonate platform facies to more distal, slope and basinal facies, similar to that observed in the Middle Jurassic (Matias 2007)
Middle Jurassic	Onshore, sediments are mainly limestone, sometimes calciclastic, and marly limestone to marls (Terrinha *et al.* 2006). Offshore, dolomites (Imperador-1; western sector) evolving to marls (Algarve-1; eastern sector) are the most common. Variation in these lateral facies is interpreted as a change from the carbonate platform facies in the west to deeper shelf-slope facies towards the east (Matias 2007)
Early Jurassic	Mainly limestone and marly limestones were deposited and subsequently dolomitized during diagenesis (Ribeiro and Terrinha 2007). This was followed by a differentiation of the depositional environments, with inner-mid neritic and more pelagic areas of deposition (Matias 2007)
Late Triassic–Hettangian	Red fluvial sandstones interlayered with shales and conglomerates, capped by Hettangian pelite–carbonate–evaporite complexes (Lopes *et al.* 2006). This latter unit was identified in the Ruivo-1 well (western sector), and is composed primarily of anhydrite with minor interbedded claystone layers, limestone and salt. During the Late Sinemurian the margin evolved from fluvial to estuarine and floodplain conditions, followed by an uplift episode associated with basaltic volcanism (Terrinha 1998)

a complex Mesozoic record marked by differences in the lithostratigraphy due to episodes of east–west segmentation that occurred as an effect of the tectonic evolution of the North Atlantic and the Tethys oceans. The stratigraphy of the Algarve Basin is based on outcrop observation and commercial well data. A summary description of the main basin lithologies is presented in Table 4.

Methods and materials

Data description

The CO_2 site screening assessment in Portugal was completed using the DGEG (National Directorate for Energy and Geology) database, which is the most reliable source with regard to the deep geology of the sedimentary basins in Portugal. Both the onshore and offshore settings are well covered by 2D seismic surveys (Fig. 2b), and the database comprises 174 boreholes, of which 146 are located onshore (48 are deeper than 1000 m) and 27 are located offshore (all deeper than 1000 m). Most of this database is composed of legacy data from petroleum exploration, and relevant information routinely acquired with recent techniques is often lacking (e.g. reduced set of well logs), while in some cases the data quality is low (e.g. old 2D seismic surveys). In recent years, the database was updated with new geophysical surveys (2D seismic, 3D seismic and aeromagnetic surveys) for petroleum exploration, as well as new boreholes drilled onshore (Fig. 2c). Results of these recent surveys and boreholes (e.g. 3D seismic data and new onshore boreholes) are currently being included in the site screening process.

Screening criteria

The selection of sites for storing significant volumes of CO_2 involves progressively more detailed geological assessments. The identification of potential storage regions in mainland Portugal was conducted through the application of screening criteria at a basin scale to identify the suitable sedimentary basins and at a regional scale to characterize the potential reservoirs.

The criteria used for the basin-scale assessment in Portugal were adapted from the CO2CRC (2008) extended list. Among the 13 original parameters, some are not relevant or applicable in the Portuguese context. For instance, the criterion associated with the hydrocarbon potential does not apply to the sedimentary basins, as there are no hydrocarbon exploitation fields in Portugal based on exploration studies conducted during the last decades. Other original criteria such as climate (moderate), accessibility (easy/accessible) and infrastructures for CO_2 storage (inexistent) are examples of criteria discarded for this assessment due to the general similarity of all the sedimentary basins and, therefore, do not allow differentiation between different areas of the basins. Table 5 presents the seven final criteria used as guidelines for the assessment of sedimentary basins in Portugal.

The regional-scale assessment conducted in the COMET project followed a set of criteria (Martinez *et al.* 2010) that considered several geological constraints such as: occurrence of supercritical conditions, geometry of the reservoir, permeability and porosity of the reservoir, salinity of the formation water, thickness and continuity of the cap rock, and existence of known active faults. Table 6 lists these relevant properties grouped in three key parameters: storage capacity, injectivity and integrity of seal. The storage capacity is directly influenced by the effective pore volume, trap type and supercritical conditions of CO_2. As a general rule, for instance, the regional-scale assessment only considers storage depths of less than 2500 m; although some greater depths could be accepted if well argued by geologists. Moreover, the screening assessment accounts for the structures and formations at depths of $\geq$800 m as the CO_2 must be injected under supercritical conditions (i.e. 800–900 kg m^{-3}) to make the storage economically viable. The injectivity depends greatly on the trap type and petrophysical properties (permeability and porosity) of the storage unit. Among several relevant properties regarding the integrity of the seal, the permeability, thickness and homogeneity are key properties that determine the effectiveness of the cap rock (Martinez *et al.* 2010).

Reservoir and cap-rock properties

The estimation of the petrophysical properties, namely permeability and porosity but also relevant reservoir parameters such as the net/gross and salinity, are crucial for an adequate formation evaluation of reservoirs and cap rocks for CO_2 geological storage. The porosity is directly related to the storage capacity of the reservoir through the effective pore volume, which ideally should exhibit not only high porosity values but also a good interconnection between the rock pores. The permeability directly influences the injectivity of CO_2 into the reservoir since it is a measure of the ability of the sedimentary rock to transmit fluids along the aquifer. Permeability is also a relevant parameter associated with the cap rock, which should present very low values.

Porosity values were estimated from several available geophysical logs in oil exploration boreholes, such as sonic logs, compensated neutron logs (CNL) and sidewall neutron logs

Table 5. *Criteria for screening sedimentary basins (adapted from CO2CRC 2008)*

	Increasing CO_2 storage potential →				
	Classes				
Criterion	1	2	3	4	5
Seismicity (tectonic setting)	Very high (e.g. subduction)	High (e.g. synrift, strike slip)	Intermediate (e.g. foreland)	Low (e.g. passive margin)	Very low (e.g. cratonic)
Size	Very small (<1000 km^2)	Small (1000–5000 km^2)	Medium (5000 – 25 000 km^2)	Large (25 000–50 000 km^2)	Very large (>50 000 km^2)
Depth	Very shallow (<300 m)	Shallow (300–800 m)		Deep (>3500 m)	Intermediate (800–3500 m)
Faulting intensity	Extensive		Moderate		Limited
Hydrogeology	Shallow, short-flow systems or compaction flow				Regional, long-range flow systems; topography or erosional flow
Geothermal	Warm basin (>40°C km^{-1})				Cold basin (<30°C km^{-1})
Reservoir–seal pairs	Poor		Intermediate		Excellent

Table 6. *Screening criteria applied in the COMET project (compiled after Martinez et al. 2010)*

Key parameters	Properties	Description
Storage capacity	Porosity	Preferably >15% 6–15%, considered depending on other parameters
	Trap type	Traps and regional reservoirs
	Effective pore volume	Storage capacities >3 Mt
	Depth of reservoir	Reservoir top is from 800 to 2500 m deep
Injectivity	Trap type	Open traps/reservoirs are favoured over closed traps/reservoirs
	Permeability	Preferably >200 mD
	Rock mechanics, diffusivity	Account for geomechanical and diffusivity parameters Maximum pressure 20% initial pressure
Integrity of seal	Permeability	Maximum permeability 2–10 mD
	Seal thickness	Preferably >50 m
	Faulting and tectonic activity	Less faulted formations are favoured Seismo-tectonic behaviour is considered Discard formations/traps crossed by active faults
	Homogeneity of seal	Homogeneous and laterally continuous formations are favoured

(SNL). Porosity profiles of several wells located in the four sedimentary basins of the study were converted from sonic logs to porosity values using the Wyllie time-average equation (Wyllie *et al.* 1958; Martinez 2013).

The net/gross values were based on analyses of geophysical logs and lithostratigraphic columns described in previous research (Palin 1976; Barbosa 1981; Marques da Silva 1990, 1992).

To estimate the water salinity of potential reservoirs, electrical logs (i.e. induced resistivity and laterolog logs) were interpreted from available petroleum exploration boreholes that intercepted the depths of interest; based on Archie's law (Archie 1942; Winsauer *et al.* 1952), water resistivity was estimated and correlated with equivalent NaCl (Keys 1990; Chappelier 1992; Schlumberger 2009).

Permeability measurements are almost completely absent in the legacy wells from petroleum exploration at the required depths of CO_2 storage. Permeability was estimated from 222 groundwater wells that intersect the same formations at shallower depths. From the available 222 wells, 79 were used for this study because their screens were placed in the geological formations coinciding with potential reservoirs and because pumping tests provided evidence of steady-state dynamic water levels. The data were extrapolated to the reservoir depths using a fit approach to the permeability–depth curve and are only presented for the onshore reservoirs.

Definition of storage units

After identifying pairs of potential reservoirs–cap rocks, 2D seismic lines from the database illustrated in Figure 2b were used to define the storage units for each sedimentary basin. Based on 2D seismic interpretation, structural maps in two-way time (TWT) were generated from the horizons of different chronostratigraphic sequences, and were subsequently converted into depth (metres) using velocity models built accordingly (from sonic logs) for the several basins of this study. After the time–depth conversion, zones restricted to the supercritical conditions of CO_2 were identified from the structural maps in depth, allowing for the definition of the storage units. In addition, it is important to mention that the fault networks were interpreted from seismic data and also used to delineate the different areas of potential injection. The resulting data from seismic interpretation were integrated into a GIS (geographical information system) platform to generate the final storage units for each basin.

Storage capacity estimate

The storage capacity of the potential injection sites was estimated using the volumetric approach (Vangkilde-Pedersen *et al.* 2009), in which regional storage capacity (M_{CO_2}) is calculated using equation (1). This formulation was proposed in 2007 by the Carbon Sequestration Leadership Forum (CSLF) for effective storage capacity in basin- and regional-scale assessments, and was previously applied in the EU GEOCAPACITY project (Vangkilde-Pedersen *et al.* 2009):

$$M_{CO_2} = A\,h\,NG\,\phi\,\rho_{CO_2 r} S_{eff} \quad (1)$$

where A is the area of trap (or regional aquifer); h, NG and ϕ are the average values for thickness, net/gross ratio and porosity of the reservoir, respectively; $\rho_{CO_2 r}$ is the CO_2 density at reservoir conditions; and S_{eff} is the storage efficiency factor. The source of data associated with each parameter of equation (1) is indicated in Table 7.

The storage efficiency factor (S_{eff}) is the main source of uncertainty since it is site specific and needs to be determined through numerical simulations (Cavanagh *et al.* 2020), or at least from the rock and fluid compressibility and admissible pressure

Table 7. *Parameters used in the storage capacity calculation and sources of data*

Parameter	Units	Data source
A	km^2	Evaluated with GIS for each individual area with regard to the existence of supercritical conditions. GIS layers include: depth maps of the top and bottom of the reservoir, built from the interpretation of 2D seismic; hydrostatic pressure maps; geothermal gradient; and surface and seabed temperature maps
h	m	Evaluated with GIS for each individual area from isopach maps of the reservoir. In equation (1), this parameter was used as the thickness at the location of an existing borehole or, in the absence of boreholes, at the centroid of the polygon delimiting the area
NG	% (or decimal)	Evaluated from lithology records of the boreholes in, or nearest, to each individual area
ϕ	% (or decimal)	Evaluated from geophysical logs in boreholes in, or nearest, to each individual area
$\rho_{CO_2 r}$	kg m^{-3}	ECO2N data (CO2TAB) of CO_2 properties for the reservoir pressure (hydrostatic) and temperature estimated using GIS
S_{eff}	% (or decimal)	Varying the values according to semi-closed aquifers (Cavanagh *et al.* 2020)

increase (Goodman *et al.* 2011). To overcome this difficulty, an initial approach of using a constant and conservative value of S_{eff} = 2% was adopted. However, including a comparison to storage efficiency factors, proposed by Cavanagh *et al.* (2020) for a regional-scale assessment in clastic reservoirs, the use of S_{eff} = 2% lies between the P_{10} and P_{50} values of a semi-closed aquifer. In fact, most study areas and potential storage units presented in this work are bounded by faults; however, there is a lack of information about their hydraulic behaviour to effectively classify the DSA resources in open or closed aquifers and, consequently, to compartmentalize the potential reservoirs. Therefore, the storage capacity of every potential area was calculated assuming that the storage units are semi-closed aquifers, varying the S_{eff} accordingly (Cavanagh *et al.* 2020) and incorporating the uncertainty of this parameter into the storage estimates. According to the pyramid classification of the maturation of storage resources (CSLF 2007) (Fig. 7a), Cavanagh *et al.* (2020) proposed the classification of Tier 1 (T1: i.e. the low-matured level is classified) for the first assessment to estimate the storage capacity of geological formations and storage units using generic values of S_{eff}. Tier 2 (T2) consists of the discovery assessment, encompassing the estimation of storage capacity of daughter units (i.e. suitable reservoirs) based on tailored S_{eff} values. Thus, storage efficiency factors (Fig. 7b) of S_{eff} = 0.75% (P_{90}), S_{eff} = 1.5% (P_{50}) and S_{eff} = 3% (P_{10}) were assigned to the potential sites of maturity level Tier 1 (offshore sites), while for sites of maturity level Tier 2 (onshore sites) values of S_{eff} = 0.7% (P_{90}), S_{eff} = 1.5% (P_{50}) and S_{eff} = 2.8% (P_{10}) were used (Cavanagh *et al.* 2020).

Clustering of storage sites

For the sake of simplifying the analysis of potential storage units and the definition of CO_2 transport logistics (i.e. network options, risks and costs), storage clusters were adopted to aggregate multiple potential areas. The clustering approach was based on three criteria:

(a) Continuity of geological basin/structure: potential storage areas were included in the same cluster when multiple areas belonged to the same sedimentary basin, and there was the possibility that injected CO_2 may spread across contiguous areas.

(b) Distance between selected areas: distance between potential injection sites was considered, although no constant distance was imposed. For each selected area, the potential injection site was defined as the location of an existing borehole or, in the absence of boreholes, as the centroid of the polygon limiting the selected area. Similar to criterion (a), several clusters may still result in the same basin if the injection sites were too distant from each other.

(c) Onshore /offshore setting: onshore and offshore potential storage areas were always included in distinct clusters, even if there was geological continuity between them. This criterion was imposed due to different logistics (i.e. cost-effectiveness) involved in onshore and offshore storage.

Results

The basin-scale criteria described in Table 5 was instrumental in determining the promising sedimentary basins in Portugal (Martinez 2013). Among the four basins screened (Fig. 2a), the Porto, Lusitanian (including the southernmost sector Alentejo Basin) and Algarve basins achieved an overall high classification as sedimentary basins with potential to proceed with feasibility studies of CCS. Conversely, the Tejo-Sado Basin, developed onshore (Fig. 2a), was rejected as a potential region for geological storage of CO_2 due to the existence of groundwater resources used for public water supply, unsuitable nature of cap rocks, neotectonics and seismicity, and the geological structure (Machado *et al.* 2007; Martinez 2013). Therefore, based on these constraints, and despite the favourable geographical location of the Tagus-Sado Basin close to many CO_2 emission sources, it was discarded as a possibility for

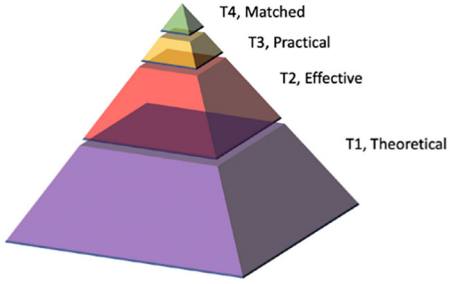

(a)

Matched / Justified			P_{90}	P_{50}	P_{10}
Tier 4	Sites	Model	Simulation	Simulation	Simulation

Practical / Contingent			P_{90}	P_{50}	P_{10}	P_{90}	P_{50}	P_{10}	P_{90}	P_{50}	P_{10}
Local			CLOSED	CLOSED	CLOSED	SEMI	SEMI	SEMI	OPEN	OPEN	OPEN
Tier 3	Prospects	Clastics	0.5	1.4	3.3	1.8	3.7	6.7	3.1	6.1	10
		Dolomites	0.9	1.5	3.1	3.0	4.2	6.1	5.1	6.9	9.2
		Limestones	0.6	1.2	2.4	2.0	3.2	4.9	3.5	5.2	7.3
		Global	0.4			4			8		

Effective / Prospective			P_{90}	P_{50}	P_{10}	P_{90}	P_{50}	P_{10}	P_{90}	P_{50}	P_{10}
Regional			CLOSED	CLOSED	CLOSED	SEMI	SEMI	SEMI	OPEN	OPEN	OPEN
Tier 2	Daughters	Clastics	0.2	0.5	1.4	0.7	1.5	2.8	1.2	2.4	4.1
		Dolomites	0.3	0.6	1.2	1.2	1.7	2.4	2.0	2.7	3.6
		Limestones	0.2	0.4	0.9	0.8	1.2	1.9	1.3	2.0	2.8
		Global	0.2			2			4		

Theoretical / Exploration			P_{90}	P_{50}	P_{10}	P_{90}	P_{50}	P_{10}	P_{90}	P_{50}	P_{10}
Regional			CLOSED	CLOSED	CLOSED	SEMI	SEMI	SEMI	OPEN	OPEN	OPEN
Tier 1	Formations	Units	0.2	0.5	1.0	0.75	1.5	3.0	1.0	2.5	5.0
		Global	0.1			1			2		

(b)

Fig. 7. (**a**) Four-tier capacity pyramid with CSLF terminology. (**b**) Storage efficiency factors as percentages for deep saline aquifers at different levels of maturity (adapted from Cavanagh *et al.* 2020).

CO_2 storage. The following subsections focus only on the regional-scale screening and characterization of the Porto, Lusitanian, Alentejo and Algarve basins, covering the estimates of petrophysical properties (Fig. 8; Table 8) and formation evaluation (i.e. the definition of reservoir–cap rock pairs), the storage site capacity (Tables 8 and 9), and the source–storage site match.

Porto Basin

Lithological and geophysical logs from three exploration wells (5A-1, Touro-1 and Lima-1) were analysed to distinguish between potential reservoirs and caprocks. From the simplified porosity-depth profiles (Fig. 8a–c), two geological formations stand as potential reservoirs for CO_2 storage:

- The Torres Vedras Group (seismic units K1–K2 in Fig. 3), with porosities ranging from 20 to 40% and thickness varying from 160 m to almost 1000 m, which is sealed by the Cacém Formation (seismic units K3/C1–C4 in Fig. 3) that is generally less than 100 m thick, with porosities of around 10%. According to Table 1, the reservoir is characterized by coarse quartz sandstones, grading to conglomerates, intercalating with fine-grained quartz sandstones, sandy clays and marls, capped by limestones, marly and argillaceous dolomites, and dolomitic limestones.
- The Silves Group (seismic unit T-J1 in Fig. 3), which exhibits porosities of up to 20% and thicknesses greater than 800 m, sealed by low-porosity sediments of the Dagorda Formation (seismic units J1–J2 in Fig. 3). Based on the lithostratigraphic table of this basin (Table 1), the potential reservoir is mainly composed of sandy-conglomeratic sediments, and the cap rock is characterized by evaporitic sediments with intercalations of clays, limestones, mudstones and anhydrite.

Salinity estimations were based on geophysical logs from the well Touro-1 for the depth interval corresponding to Torres Vedras Group, with values of *c.* 15 g l^{-1} of equivalent NaCl. Although this information is lacking from other wells in this basin, salinity values ranging higher than 10 g l^{-1} of equivalent NaCl could be found in the potential reservoir area intercepted by well Lima-1. The net/gross parameter was estimated (from well Cavala-4) as *c.* 37% for the potential reservoirs in the Torres Vedras Group; a value of *c.* 25% for the reservoir in the Silves Group was adopted from the interpretation of lithostratigraphic columns by Palin (1976), based on the same geological formation located at the northern Lusitanian Basin.

The areas with suitable conditions for supercritical behaviour of CO_2 were estimated based on the hydrostatic pressure and geothermal gradient maps for the Torres Vedras Group and for the Silves Group potential reservoir. However, in the latter, only a narrow band sub-parallel to the coast was deemed appropriate for CO_2 storage, since a maximum depth of 2500 m was imposed as an economic threshold for CO_2 storage. Figure 9a illustrates the eight storage units associated with the Torres Vedras Group (Q1-TV1, Q1-TV2, Q1-TV3, Q1-TV4, Q2-TV1, Q2-TV2, Q2-TV3 and Q2-TV4), and Figure 8b shows the storage unit defined for the reservoir of the Silves Group (Q2-S1). The resulting petrophysical properties (average values) for all storage units of this basin are presented in Table 8.

Lusitanian Basin

The porosity values regarding potential reservoirs on the offshore Lusitanian Basin (North and Central sectors) were estimated from geophysical logs in five exploration wells (Do-1, Mo-1, Fa-1, 16A-1 and 17C-1). Most of these wells do not reach the Variscan basement and, in places, there are gaps in the sedimentary record (i.e. no core recovery) and/or in the sonic log record (Fig. 8d–h).

It is also worth highlighting that the formations exhibit a considerable variation in thickness along the basin, namely at the structural highs where most wells have been drilled. From the simplified porosity–depth profiles, two formations stand out as potential storage reservoirs:

- The Torres Vedras Group (seismic unit K20 in Fig. 4), with porosities ranging between 15 and 40%. The Torres Vedras Group is topped by the Cacém Formation (seismic unit K20b–K40 in Fig. 4), with values of porosities of the order of 15%. Similar to the Porto Basin, these reservoirs are composed of siliciclastic sediments, predominantly sandstones, sealed mainly by limestones (Table 2). The Cacém Formation is the primary cap rock. In the onshore setting, and where the Torres Vedras Group is normally a relevant freshwater aquifer, it acts as a confined aquifer resulting from facies variations in the vertical sequence of the Torres Vedras Group itself, which contributes to the safety of the storage complex.
- The Silves Group (seismic unit J10 in Fig. 4) exhibits porosities of up to 15–25% and is sealed by low-porosity sediments of the Dagorda Formation (seismic unit J10–J20 in Fig. 4). For both onshore and offshore settings, these potential reservoirs are characterized by siliciclastic deposits (sands and sandy-conglomeratic sediments) capped by evaporites (halite) with intercalations of dolomitic shales and anhydrite (Table 2).

The net/gross parameter for the offshore Lusitanian Basin was assessed using information available in the logs of several boreholes for the Torres Vedras Group potential reservoirs, with estimated values of *c.* 35 (13C-1, 14C-1A and Fa-1), 66 (Ca-1, Mo-1 and 13E-1), 94 (Do-1C) and 62% (16A-1). Furthermore, it was possible to estimate the net/gross parameter for the same formation in the onshore setting through the interpretation of lithostratigraphic columns (Barbosa 1981; Marques da Silva 1990, 1992) with values of *c.* 77%, and from boreholes (MRW-5, MRW-8, MRW-9 and SPM-2) with values of *c.* 70%. For reservoirs in the Silves Group, no clarifying information was available from offshore wells, and values of *c.* 25% were adopted from the equivalent onshore geological formations, estimated from the interpretation of lithostratigraphic columns in Palin (1976). Regarding salinity estimations for the Torres Vedras Group, values of equivalent NaCl were estimated as *c.* 45 (well Mo-1), 18 (Do-1C), 130 (Fa-1), 75 (16A-1) and 10 g l^{-1} (13E-1). Despite the sparse information related to potential Silves Group reservoirs, salinity values were estimated as 9 (Fa-1), 40 (17C-1) and 10 g l^{-1} (Ca-1) of equivalent NaCl.

Eight closed storage sites (Fig. 10a) were defined for the Torres Vedras Group (designated as Q3-TV1, Q3-TV2, Q3-TV3, Q3-TV4, Q3-TV5, Q4-TV1, Q6-TV1 and Q6-TV2) and five potential areas (Fig. 10b) were defined for the Silves Group (Q3-S1, Q3-S2, Q4-S1, Q6-S1 and Q6-S2).

The Torres Vedras Group has either been eroded in much of the onshore sector of the Lusitanian Basin or occurs too shallow (i.e. <800 m) for CO_2 storage. Therefore, the Torres Vedras Group is not an adequate reservoir in the onshore sector of the Lusitanian Basin. Thus, the only potential reservoir is the Silves Group (Upper Triassic). Four areas were defined as having potential for CO_2 storage: (a) São Mamede; (b) Alcobaça; (c) São Pedro de Moel and (d) Alvorninha (Figs 10b and 11a). Several faults with cartographic expression intercept the reservoir (Fig. 11b), apparently highly compartmentalized. However, there are no indications as to the hydraulic behaviour of these faults. An excellent seal caps the

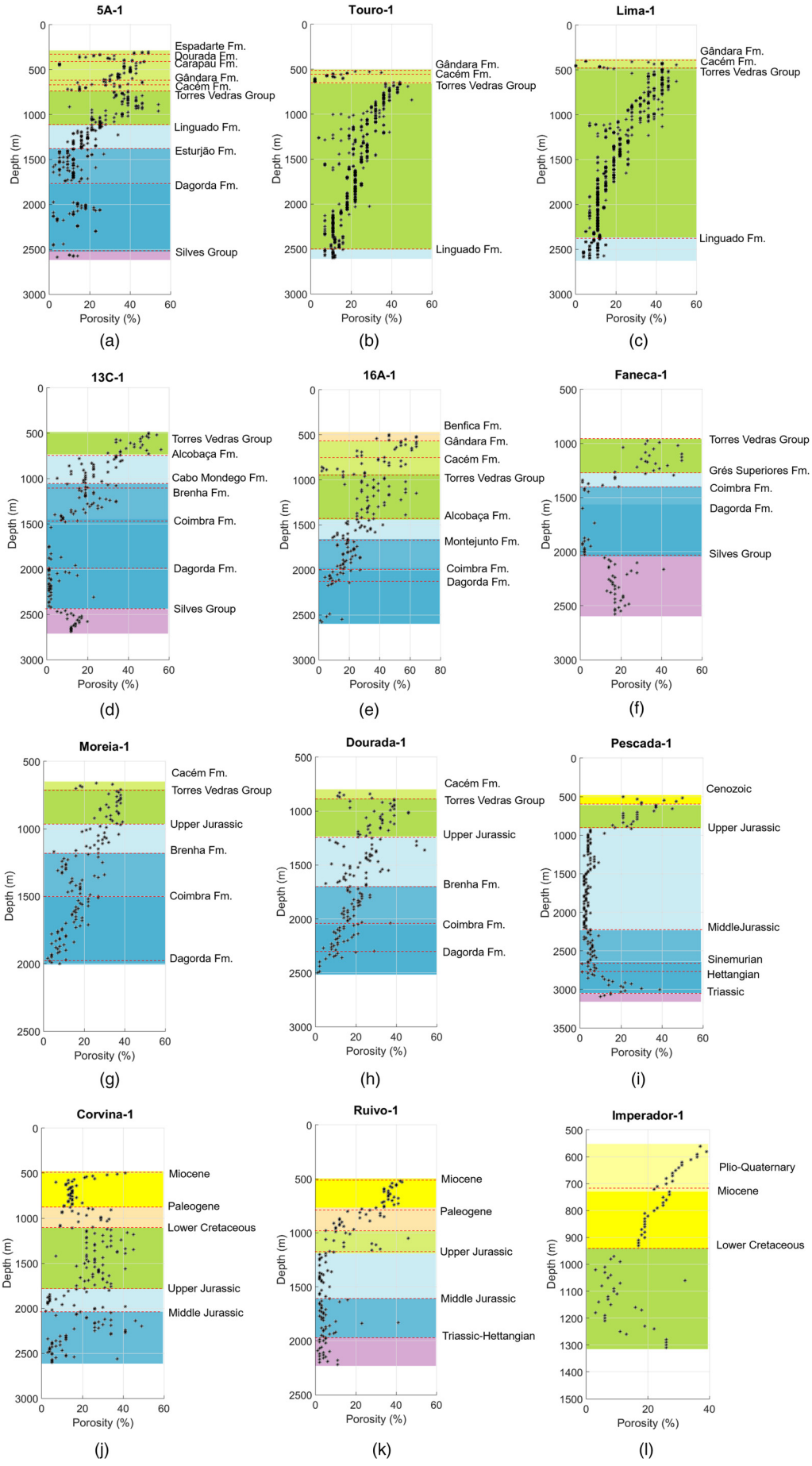

Fig. 8. Porosity v. depth from boreholes located in the (**a**)–(**c**) Porto Basin, (**d**)–(**h**) Lusitanian Basin, (**i**) Alentejo Basin and (**j**)–(**l**) Algarve Basin.

Table 8. *Database of reservoir properties and storage capacity in the selected areas of each basin*

Basin	Storage unit	A	h	NG	ϕ	ρ_{CO_2r}	S_{eff}	M_{CO_2}
Porto	Q1-TV1	448	645	0.37	0.25	787	0.015	316
	Q1-TV2	429	887	0.37	0.25	728	0.015	384
	Q1-TV3	290	607	0.37	0.25	509	0.015	124
	Q2-TV1	218	306	0.37	0.25	664	0.015	61
	Q2-TV2	166	284	0.37	0.25	539	0.015	35
	Q2-TV3	993	319	0.18	0.25	683	0.015	146
	Q1-TV4	636	445	0.37	0.25	723	0.015	284
	Q2-TV4	343	421	0.37	0.25	644	0.015	129
	Q2-S1	873	433	0.25	0.10	709	0.015	251
	Porto Basin – total storage capacity (Mt CO_2)							**1731**
Lusitanian	Q3-TV1	696	327	0.66	0.30	668	0.015	452
	Q3-TV2	509	274	0.66	0.30	648	0.015	268
	Q4-TV1	407	349	0.66	0.30	567	0.015	239
	Q3-TV4	640	237	0.35	0.30	664	0.015	159
	Q3-TV5	387	303	0.35	0.30	642	0.015	119
	Q3-TV3	541	369	0.94	0.30	630	0.015	532
	Q6-TV1	243	365	0.35	0.30	572	0.015	80
	Q6-TV2	1125	345	0.62	0.30	709	0.015	768
	Q4-S1	551	387	0.56	0.15	671	0.015	180
	Q3-S1	624	216	0.25	0.15	676	0.015	51
	Q3-S2	82	245	0.25	0.15	639	0.015	7
	Q6-S1	60	352	0.25	0.15	661	0.015	8
	Q6-S2	23	403	0.25	0.15	679	0.015	4
	North and Central Lusitanian Basin – total storage capacity (Mt CO_2)							**2867**
	São Mamede	292	1300	0.25	0.13	738	0.015	137
	Alcobaça	159	1234	0.25	0.13	667	0.015	64
	São Pedro de Moel	158	802	0.25	0.13	614	0.015	38
	Alvorninha	76	873	0.25	0.13	639	0.015	21
	Onshore Lusitanian Basin – total storage capacity (Mt CO_2)							**260**
Alentejo	Q10-S1	230	100	0.62	0.10	775	0.015	17
	Q10-S2	211	100	0.62	0.10	710	0.015	14
	Q9-S1	367	100	0.62	0.10	645	0.015	22
	Q10-S3	219	100	0.62	0.10	535	0.015	11
	Alentejo Basin – total storage capacity (Mt CO_2)							**64**
Algarve	Q16-TV1	135	437	0.40	0.20	721	0.015	51
	Q16-TV2	213	768	0.40	0.20	803	0.015	158
	Q16-TV3	58	584	0.35	0.20	798	0.015	28
	Q16-TV4	109	709	0.35	0.20	794	0.015	64
	Q15-TV1	3075	585	0.35	0.20	726	0.015	1371
	Q15-M1	3021	196	0.25	0.30	746	0.015	497
	Algarve Basin – total storage capacity (Mt CO_2)							**2169**
Total storage capacity in Portugal (Gt CO_2)								**7.09**

reservoir, composed of salt, clay and marls of the Lower Jurassic Dagorda Formation, with thickness values usually greater than 400 m and occasionally thicker than 1500 m in the São Mamede and Alcobaça areas. In the Alvorninha area, the thickness is less than 200 m.

Reservoir porosity and the salinity of the formation water were assessed using geophysical logs from wells Aljubarrota-2 (Alj-2: Fig. 11b) and Aljubarrota-1 (Alj-1/1A: Fig. 11b) located in the São Mamede and Alcobaça sites, respectively (Pereira *et al.* 2014). The porosity is low, ranging from 3 to 9%; the estimated values of

Table 9. *Main features of storage clusters*

Cluster ID	Sedimentary basin	Setting	No. of selected areas	Site IDs	Cluster storage capacity (Mt CO_2)
S01	Porto	Offshore	5	Q1-TV1, Q1-TV2, Q1-TV3, Q2-TV1 and Q2-TV2	921
S02	Porto	Offshore	4	Q2-TV3, Q1-TV4, Q2-TV4 and Q2-S1	810
S03	Lusitanian (north sector)	Offshore	5	Q3-TV1, Q3-TV2, Q4-TV1, Q3-TV3 and Q4-S1	1671
S04	Lusitanian (north sector)	Offshore	8	Q3-TV4, Q3-TV5, Q6-TV1, Q6-TV2, Q3-S1, Q3-S2, Q6-S1 and Q6-S2	1196
S05	Lusitanian (north and central sectors)	Onshore	4	São Mamede, Alcobaça, São Pedro de Moel and Alvorninha	260
S06	Alentejo	Offshore	4	Q10-S1, Q10-S2, Q9-S1 and Q10-S3	64
S07	Algarve	Offshore	4	Q16-TV1, Q16-TV2, Q16-TV3 and Q16-TV4	301
S42	Algarve	Offshore	2	Q15-TV1 and Q15-M1	1868

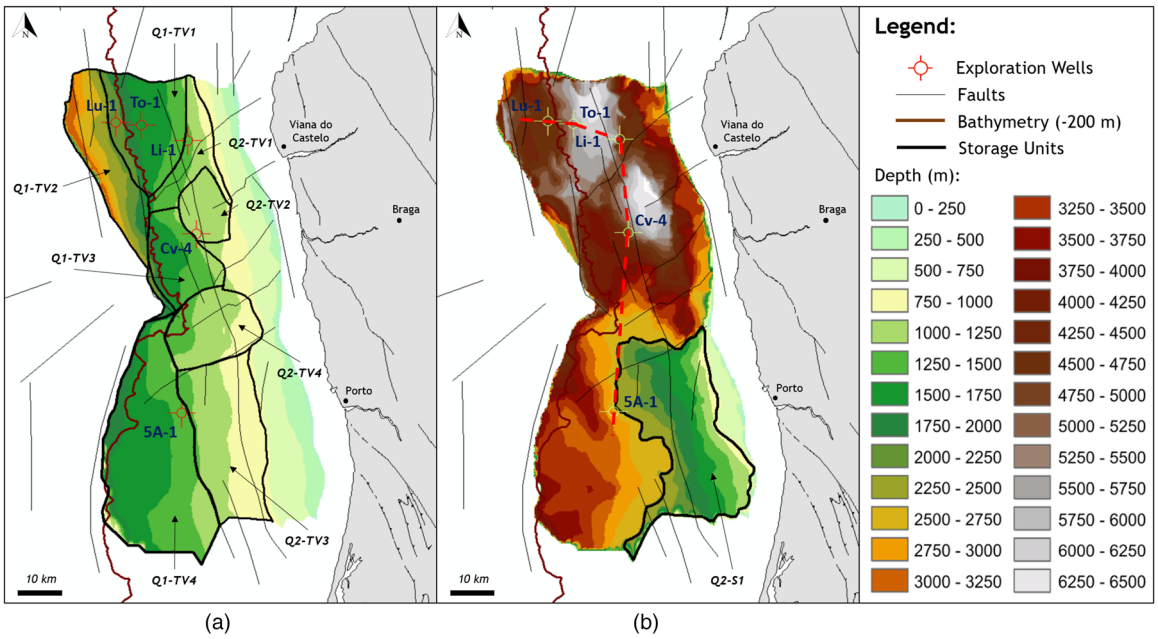

Fig. 9. Structural maps illustrating the location of exploration wells and selected areas for CO_2 geological storage: (**a**) potential reservoirs within the Torres Vedras Group and (**b**) potential reservoirs within the Silves Group. The red dashed line corresponds to the cross-section in Figure 3. See Figure 1b for the location of this study area in Portugal.

salinity were higher than 10 g l^{-1} of equivalent NaCl. Regarding the net/gross parameter, values of *c.* 56 and 25% were estimated from the interpretation of several lithostratigraphic columns in Palin (1976). The resulting petrophysical properties (average values) for all storage units of this basin are presented in Table 8.

The permeability was estimated in the onshore reservoir formation (i.e. Silves Group) using 10 samples, and ranges between 67 and 783 mD for the average well screen depths of 44–275 m. The average value of permeability was 358 mD, and 60% of the results were above 300 mD. Regarding the geological formations of the Torres Vedras Group, the permeability was estimated, using 69 samples, to range between 129 and 19570 mD for the average well screen depths of 32.5–243.5 m. The average value of permeability was 2235 mD and 94% of the results were above 300 mD.

Alentejo Basin

In the shallow offshore of the Alentejo Basin (southernmost sector of the Lusitanian Basin), the porosity of formations was estimated from one well (Pescada-1). From the simplified porosity–depth profile (Fig. 8i), the Silves Group (Triassic: Fig. 5) strikes as being of possible interest for CO_2 storage, characterized by siliciclastic deposits (Table 3: mainly red sandstones with intercalations of conglomeratic and pelitic sediments), with porosities ranging from 15 to 25% and sealed by the low-porosity sediments (Table 3:

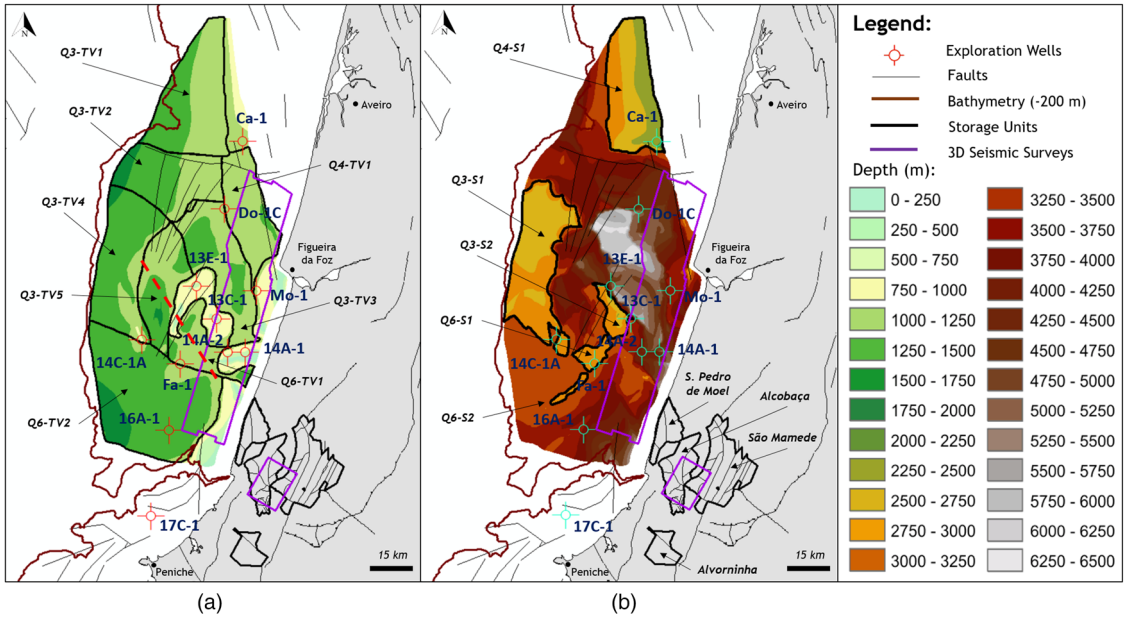

Fig. 10. Structural maps illustrating the location of exploration wells and selected areas for CO_2 geological storage: (**a**) potential reservoirs within the Torres Vedras Group and (**b**) potential reservoirs within the Silves Group. The red dashed line corresponds to the cross-section in Figure 4. See Figure 1b for the location of this study area in Portugal.

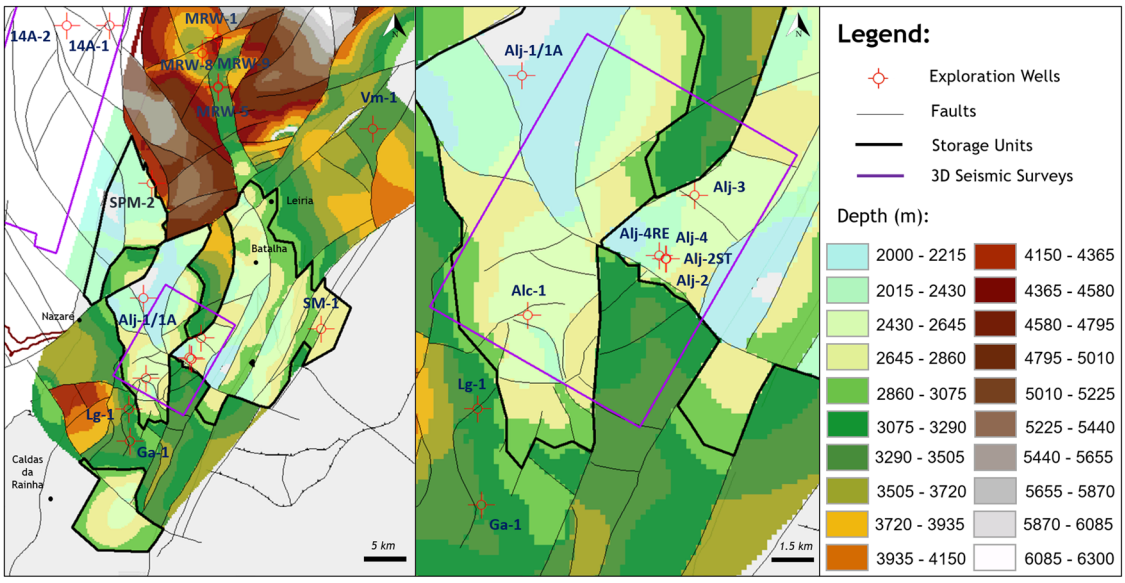

Fig. 11. Structural maps illustrating the potential reservoirs within the Silves Group: (**a**) the location of selected areas for geological storage of CO_2 and (**b**) the location of exploration wells within the 3D seismic survey partially covering both the Alcobaça and São Mamede storage sites. See Figure 1b for the location of this study area in Portugal.

mainly shales, evaporites and limestones) of the Dagorda Formation (Hettangian–Lower Jurassic units in Fig. 5). The top of the Silves Formation is in extensive areas within the ideal pressure interval for CO2 storage (Vangkilde-Pedersen *et al.* 2009), with depths ranging between 800 and 2500 m.

Considering other reservoir properties, there is no information available in the two wells that intercept the reservoir (Pe-1 and Go-1) to estimate the salinity values. Nonetheless, well Go-1 provided data to determine the net/gross of potential reservoirs to be 62%. Palin (1976) estimated the net/gross parameter at *c.* 57% from the lithostratigraphic column of this area (Santiago do Cacém).

This sector was subdivided into four storage areas (Q9-S1, Q10-S1, Q10-S2 and Q10-S3) based on the physiography of the basin and the limits associated with the fault network (Fig. 12), which may act as natural barriers for liquid/gas migration. These areas are the most favourable locations for CO_2 storage in the shallow offshore area of the Alentejo Basin, with expected siliciclastic sections in the Silves Group presenting fair–good reservoir characteristics and varying laterally in thickness. Due to its thickness and rheology, the thin evaporite coverage of the Dagorda units can act as an effective seal. Also, the argillaceous sections at the top of the Silves Group can act as good seals, if proper porosity and permeability conditions exist. The resulting petrophysical properties (average values) for all storage units of this basin are presented in Table 8.

Algarve Basin

The simplified porosity–depth profiles (Fig. 8j–l), interpreted from the geophysical logs (boreholes Corvina-1, Ruivo-1 and Imperador-1), revealed possible reservoirs in the Early Cretaceous sequence (Imperador-1 and Corvina-1) and in the base Late Cretaceous sequence (Ruivo-1), with porosities ranging from 15 to 30%. However, these sequences do not exhibit great lateral continuity. Moreover, the Cretaceous sequences are topped by Paleogene limestones, marls, clays and sands (Table 4) with highly variable porosities that do not constitute a high-quality seal.

Miocene sand layers are also possible reservoirs, with porosities ranging from 20 to 33% (Matias 2007), overlain by extensive shale deposits from the Miocene–Pliocene and providing an effective seal (Table 4). Five wells (Imperador-1, Corvina-1, Ruivo-1, Algarve-1 and Algarve-2) intercept the Miocene sands at depths of 550–950 m, with thickness varying from 250 to 400 m. Miocene sands could act as reservoirs for CO_2 storage when occurring deeper than 800 m.

The reservoir net/gross value was estimated from well logs for potential reservoirs of the Torres Vedras Group (within the Cretaceous in Fig. 6), with values of *c.* 40 (Alg-1) and *c.* 35% (Co-1), and for Miocene reservoirs (within the Neogene in Fig. 6), with values of *c.* 25% (Im-1). Due to the lack of data, no water salinity values could be estimated.

As for the other areas, several storage areas were selected with the limits imposed by the main faults and structures. Five storage areas were selected as Cretaceous reservoirs (designated as Q15-TV1, Q16-TV1, Q16-TV2, Q16-TV3 and Q16-TV4) and one site (Q15-M1) for the Miocene reservoir (Fig. 13). The resulting petrophysical properties (average values) for all storage units of this basin are presented in Table 8.

Clusters and storage capacity

The structural maps (from 2D seismic) of the seismic horizons identified as reservoirs (Figs 9–13), and considering the depth limits set in the screening criteria (Table 6) and the petrophysical properties of each storage unit (Table 8), were used to estimate the storage capacity of the identified storage units according to equation (1) and varying the S_{eff} values (Cavanagh *et al.* 2020). The resulting mean storage capacities (P_{50}) are presented in Table 8. The overall estimated storage capacity values range from 3.54 (P_{90}) to 14.14 Gt (P_{10}), with a central estimate of 7.09 Gt (P_{50}), highlighting the importance of choosing an appropriate S_{eff} given the linear dependence of storage capacity on this parameter.

According to the previously described criteria, 36 storage units in Portugal were grouped into eight clusters, one onshore and seven offshore (Fig. 14): two clusters in the Porto Basin (S01 and S02), three in the Lusitanian Basin (offshore clusters S03 and S04, and the onshore cluster S05), one in the Alentejo Basin (S06) and two in the Algarve Basin (S07 and S08). The detailed information of the resulting storage clusters is presented in Table 9 and their spatial distribution in mainland Portugal is illustrated in Figure 14.

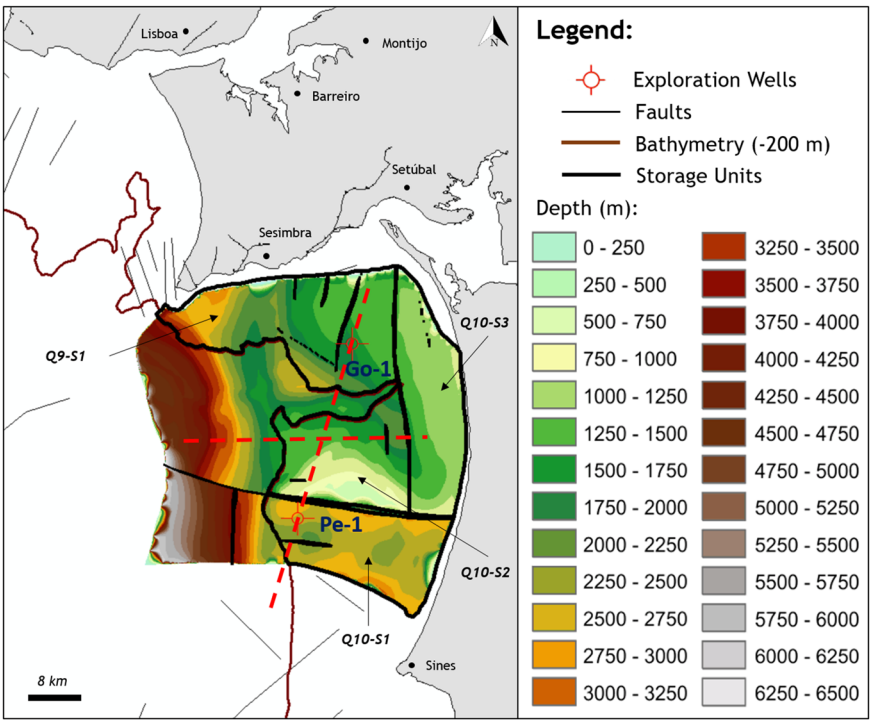

Fig. 12. Structural map illustrating the potential reservoirs within the Silves Group and the location of exploration wells. The red dashed lines correspond to the NE–SW and west–east cross-sections in Figure 5. See Figure 1b for the location of this study area in Portugal.

Discussion

The potential storage capacity in deep saline aquifers is equivalent to around 200 years of the current CO_2 emissions from stationary sources in Portugal. Since the projections made in Seixas *et al.* (2015) point to the need to store less than 10 Mt a^{-1} from 2025 to 2050, it is safe to say that Portugal has enough resources for its needs, even considering that the maturation of the analysis (i.e. rising tiers in the resources pyramid) will inevitably result in a decrease in the storage capacity estimates.

Most of the storage capacity is located in offshore storage units (P_{50}, 2.93 Gt CO_2), which contrasts with the assessed onshore capacity of only (P_{50}) *c.* 260 Mt CO_2. Most offshore storage units are located in the shallow continental shelf, close to the coast, which is a favourable location with respect to the main CO_2 sources in the country (Fig. 1).

Of the 36 areas with a potential for geological storage of CO_2, three geological formations were identified with favourable geological conditions to act as reservoirs. The youngest reservoir (Upper Miocene) is restricted to the Algarve Basin, although these sand layers are frequently shallower than the required depth to act as reservoirs. The reservoirs with the greatest storage potential belong to the Torres Vedras Group (Lower Cretaceous) within the Porto and Lusitanian basins, and the equivalent formations of the Algarve Basin, and the deeper Silves Group (Upper Triassic) within the Porto and Lusitanian basins (onshore and offshore).

Other promising geological formations were considered during the very first screening studies conducted in the KTEJO and

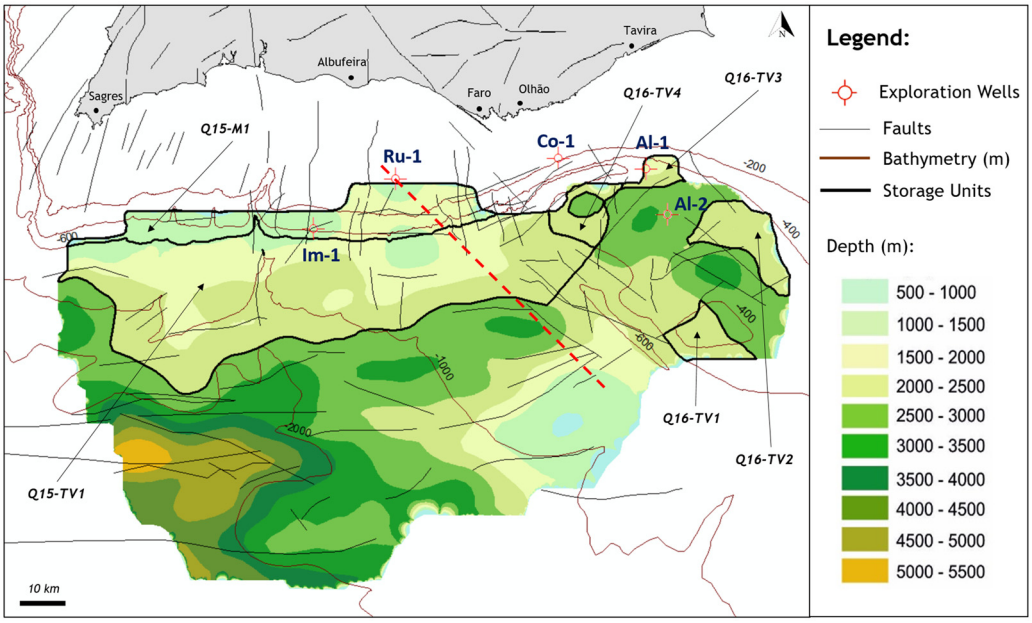

Fig. 13. Structural map illustrating the potential reservoirs (the Torres Vedras Group and Miocene sands) and the location of exploration wells in this basin. The red dashed line corresponds to the cross-section in Figure 6. See Figure 1b for the location of this study area in Portugal.

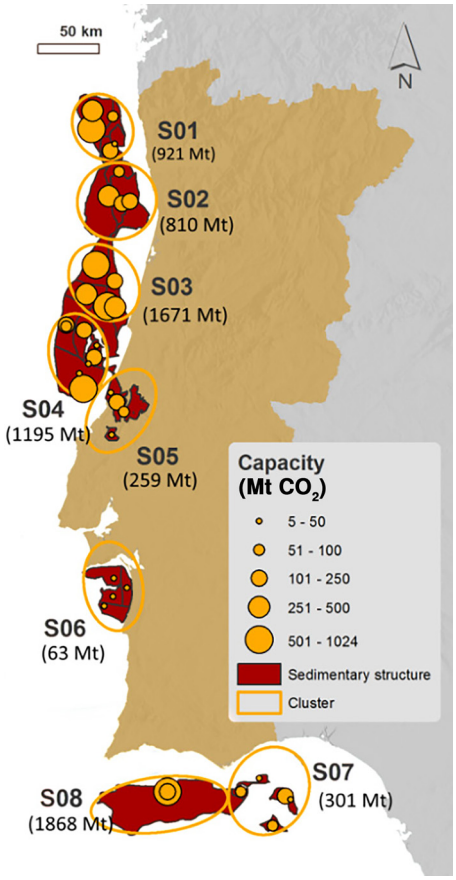

Fig. 14. Location of storage sites and capacity per cluster. The S number corresponds to cluster number; for further details refer to Table 9.

COMET projects; in particular, the Grés Superiores/Lourinhã and Alcobaça formations. In fact, these formations occur at desired depths and, in general, present favourable lithologies (Table 2). In addition, they are deeper than the potential reservoirs of the Torres Vedras Group and possibly better capped. However, the abundance of interlayered marly limestones and floodplain muds with frequent caliche deposits (Taylor *et al.* 2014) implies a greater variability in porosity values (Fig. 8d–h) and a lower net/gross ratio, which compromises the injectivity and storage capacity. Moreover, these formations present a significant variation in their lateral continuity and thickness in this basin, which corroborates the possible negative impact on the values of storage capacity.

As for the identified reservoirs and cap rocks, it must be acknowledged that the data quality is far from ideal, raising several levels of uncertainty. There is, in fact, considerable uncertainty in the quality of the Torres Vedras Group cap rock. The lower siliciclastic sequence of the Torres Vedras Group is well known onshore, where it is a very productive, confined freshwater aquifer, with clay layers within the Torres Vedras Group itself providing the confinement. Above the Torres Vedras Group, the Cacém Formation has the potential to be the primary seal but further evaluation is required.

Conversely, there is a high degree of confidence in the cap rock for the Triassic reservoir, with thick sequences, sometimes more than 1000 m, of evaporites, clays and marls in the Dagorda Formation providing excellent conditions.

Clustering the storage units, and comparing them with the sources, provides some hints about the source–sink match. Clusters within the Porto (S01 and S02) and the North Lusitanian basins (S03 and S04) present the best qualification as potential candidates for the geological storage of CO_2. Besides being located offshore and ensuring better public acceptance, they generally present higher storage capacities (Fig. 14) and are favourably located with respect to the major CO_2 source emitters (Fig. 1a), especially clusters S03 and S04.

Storage costs have been presented in Carneiro *et al.* (2015) and will be further detailed in a forthcoming paper. Concerning the northernmost clusters, the estimated storage costs (from sources to storage sites) range from €13.6 to €24.5 t^{-1} CO_2 for clusters S01 and S02, respectively. However, there are a small number of relevant CO_2 sources in that region (mainly restricted to the Porto surroundings), and the main source (a refinery) will be decommissioned in 2023. Analyses in Carneiro and Mesquita (2014) and Seixas *et al.* (2015) seem to discard storage units in cluster S02 as being too expensive to be cost-effective for sources located in northern Portugal. In the offshore setting of the Lusitanian Basin, the estimated storage costs for clusters S03 and S04 were estimated to be €12.6 and €17.3 t^{-1} CO_2, respectively. Unlike the previous clusters, S03 and S04 are cost-effective options for CO_2 storage if there is a national policy favouring offshore storage or if the onshore capacity is exhausted (Boavida *et al.* 2013; Seixas *et al.* 2015). These clusters are also favourably located with respect to the CO_2 sources and to the transport networks connecting to the onshore S05 cluster. Although the storage costs of cluster S04 are slightly higher compared to S03, this cluster is located immediately south of cluster S03 and transport costs would be lower due to its proximity to the major CO_2 emitter sources and its possible connection to the onshore cluster S05 (Boavida *et al.* 2013; Seixas *et al.* 2015).

The onshore cluster S05 presents a major advantage: it is the most cost-effective solution for the transport and storage of CO_2 from sources across most of the country (Fig. 1a: except from the CO_2 emission sources of Algarve), with estimated storage costs of *c.* €3.8 t^{-1} CO_2. Its total storage capacity is, though, significantly lower than, for instance, clusters S01, S02, S03 and S04. However, the need for storage is mostly restricted to specific industry sectors with high processing emissions, such as the cement sector, or through BECCS in biomass and waste power plants. Furthermore, the RNC2050 forecasts that by 2050 less than 10 Mt a^{-1} will remain to be abated in the industry sector, which agrees with the scenarios in Seixas *et al.* (2015). Consequently, the capacity required for the geological storage of CO_2 will not be high and may be in line with the onshore storage capacity at cluster S05, if the increase in maturity of the sites (i.e. the advancement from effective to practical capacities) does not result in a drastic decrease in the estimated capacity. The environmental and social risks associated with an onshore site are higher than that for offshore areas, and social acceptance is of crucial relevance. Note that this issue is being considered for further research development in which social acceptance of cluster S05 will be assessed by engaging with local populations and other stakeholders, and applying social science methodologies.

As for the southernmost clusters, the potential sites in cluster S06 (Alentejo Basin) are closer to the coastline and also to the main CO_2 sources in the country: that is, the Sines industrial area, and sources of the cement, paper and pulp sectors in the city of Setúbal (see Fig. 1a). Nonetheless, the estimated storage costs of *c.* €47.4 t^{-1} CO_2 (Boavida *et al.* 2013; Carneiro *et al.* 2015) are too expensive to be cost-effective, even for the nearby sources in Sines. In addition, the storage capacity is low and the Silves reservoir intercepted by petroleum boreholes in this area is more compact and has a lower permeability. Furthermore, the Alentejo Basin has a criss-cross of NE–SW active faults (Fig. 5), which run west from the potential storage area and are thought to be connected to the Nubia–Eurasia plate boundary. The issue of passive and induced seismicity is a concern for the area, and will be addressed in terms of a ranking qualification for the area in a companion paper; despite the excellent location with regard to some important sources, cluster S06 is not a priority for the geological storage of CO_2 in Portugal.

The Algarve clusters S07 and S08 present estimated storage costs of *c.* €12.2 and €10.4 t^{-1} CO_2, respectively. Although the storage costs are in line with the most cost-effective offshore clusters (e.g. S01 and S03) and present large storage capacities, they are very distant from most relevant CO_2 sources (Fig. 1a: a single relevant source in the Algarve, a cement plant in Loulé that is likely to close in the near future). Passive and induced seismicity are, once again, an issue as the Algarve region has the greatest risk of seismic activity in Portugal. Lastly, the whole economy of the Algarve is based on coastal and marine tourism, and local populations have recently reacted strongly against any drilling activity in offshore areas. Thus, CO_2 storage in clusters S07 and S08 would face a series of hurdles that could discourage deploying this activity in the region.

Conclusions

This work describes the geological studies completed for the identification and characterization of potential areas for geological storage of CO_2 in deep saline aquifers in Portugal, involving both basin- and local–regional-scale studies for screening favourable geological sites that could be considered in the future for CO_2 storage activities. The clustering approach enabled a broad overview of mainland Portugal including the storage capacity, spatial distribution of potential storage units, concerns and locations of the main emission sources, which are mainly concentrated along the Atlantic coast.

With a large potential for the geological storage of CO_2, ranging from 3.54 (P_{90}) to 14.14 Gt (P_{10}) and with a central estimate of 7.09 Gt (P_{50}), the main areas in Portugal are associated with the Lusitanian Basin, both onshore and offshore, since they are located favourably in relation to the industrial emitters of CO_2. Considering only the potential sites of this basin, they present storage capacities above 3 Gt CO_2 (*c.* 3.13 Gt CO_2), resulting in enough storage capacity for the next few decades of CO_2 stationary emissions. These are, nonetheless, estimates at the Tier 1 level for the offshore sites and at Tier 2 for the onshore sites, and a significant decrease may occur with maturity of these DSA resources. Furthermore, the data quality is far from ideal, and there is considerable uncertainty in the characterization of reservoirs and cap rocks. While the potential reservoirs in the Torres Vedras Group have better reservoir parameters (i.e. porosity, permeability and depth) for CO_2 storage, compared to the Silves Group reservoirs, there is a greater uncertainty about the quality of the identified seal (clay layers in the Torres Vedras Group and the overlying Cacém Formation). This contrasts with the excellent characteristics (e.g. thickness) of the sealing rock (Dagorda Formation) of potential reservoirs in the Silves Group.

Further work to determine uncertainties and risks, ranking qualification of storage sites, and a cost-effectiveness assessment is being conducted using recent legacy data from the petroleum exploration activities. These efforts are focusing on the Lusitanian Basin, where the storage clusters are the most promising, to move forward with detailed feasibility studies for geological storage of CO_2 in Portugal.

Acknowledgements Authors would like to thank all the institutions that have supplied data for the development of this work. In particular, we gratefully acknowledge DPEP (the Portuguese Division for Oil Exploration and Production) for providing access to technical reports and databases. We are also grateful to all COMET, KTEJO and CCS-PT project partners, and to all researchers involved in these projects. We would like to thank the two reviewers for their contribution and suggestions to improve the quality of the manuscript.

Author contributions **PP**: investigation (supporting), writing – original draft (lead), writing – review & editing (lead); **CR**: investigation (lead), project administration (supporting), writing – original draft (supporting), writing – review & editing (supporting); **JC**: investigation (supporting), project administration (lead), writing – original draft (supporting), writing – review & editing (supporting).

Funding This work was funded by the Fundação para a Ciência e a Tecnologia (grant No. UIDB/04683/2020), Fundação para a Ciência e a Tecnologia (grant No. UIDB/04292/2020) and H2020 – STRATEGY CCUS (grant No. 837754).

Data availability The data that support the findings of this study are available from the National Directorate for Energy and Geology but restrictions apply to the availability of these data, which were used under licence for the current study, and so are not publicly available. Data are, however, available from the authors upon reasonable request and with permission of the National Directorate for Energy and Geology.

References

Alves, T.M. and Cunha, T.A. 2018. A phase of transient subsidence, sediment bypass and deposition of regressive–transgressive cycles during the breakup of Iberia and Newfoundland. *Earth and Planetary Science Letters*, **484**, 168–183, https://doi.org/10.1016/j.epsl.2017.11.054

Alves, T.M., Gawthorpe, R.L., Hunt, D.W. and Monteiro J.H., 2002. Jurassic tectono-sedimentary evolution of the Northern Lusitanian Basin (offshore Portugal). *Marine and Petroleum Geology*, **19**, 727–754, https://doi.org/10.1016/S0264-8172(02)00036-3

Alves, T.M., Manuppella, G., Gawthorpe, R.L., Hunt, D.W. and Monteiro, J.H. 2003. The depositional evolution of diapir- vs. fault-bounded rift basins: examples from the Lusitanian Basin of West Iberia. *Sedimentary Geology*, **162**, 273–303, https://doi.org/10.1016/S0037-0738(03)00155-6

Alves, T.M., Moita, C., Sandnes, F., Cunha, T., Monteiro, J.H. and Pinheiro, L.M. 2006. Mesozoic–Cenozoic evolution of North Atlantic continental-slope basins: The Peniche basin, western Iberian margin. *AAPG Bulletin*, **90**, 31–60, https://doi.org/10.1306/08110504138

Alves, T.M., Moita, C., Cunha, T., Ullnaess, M., Myklebust, R., Monteiro, J.H. and Manuppella, G. 2009. Diachronous evolution of Late Jurassic–Cretaceous continental rifting in the northeast Atlantic (west Iberian margin). *Tectonics*, **28**, TC4003, https://doi.org/10.1029/2008TC002337

APA 2019. Roadmap for Carbon Neutrality 2050 (RNC2050) – Long-Term Strategy for Carbon Neutrality of the Portuguese Economy by 2050. Portugese Environment Agency, Amadora, Portugal.

Archie, G.E. 1942. The electrical resistivity log as an aid in determining some reservoir characteristics. *Transactions of the AIME*, **146**, 54–62, https://doi.org/10.2118/942054-G

Azerêdo, A.C., Duarte, L.V., Henriques, M.H. and Manuppela, G. 2003. *Da dinâmica continental no Triásico aos mares do Jurássico Inferior e Médio*. Cadernos de Geologia, Instituto Geológico e Mineiro.

Barbosa, B.P. 1981. Notícia Explicativa da Folha 16-C (Vagos). Carta Geológica de Portugal, escala 1:50 000. Serviços Geológicos, Lisbon.

Bernardes, L.F., Carneiro, J. and de Abreu, M.P. 2013. CO_2 hydrates as a climate change mitigation strategy: definition of stability zones in the Portuguese deep offshore. *International Journal of Global Warming*, **5**, 135–151, http://doi.org/10.1504/IJGW.2013.053495

Bernardes, L., Carneiro, J., Madureira, P., Brandão, F. and Roque, C. 2015. Determination of priority study areas for coupling CO_2 storage and CH_4 gas hydrates recovery in the Portuguese offshore area. *Energies*, **8**, 10 276–10 292, https://doi.org/10.3390/en80910276

Boavida, D., Carneiro, J. *et al.* 2013. Planning CCS development in the West Mediterranean. *Energy Procedia*, **37**, 3212–3220, https://doi.org/10.1016/j.egypro.2013.06.208

Boillot, G., Auxietre, J.L., Dunand, J.P., Dupeuble, P.A. and Mauffret, A. 1979. Acoustic stratigraphy and structure of the oceanic crust. *American Geophysical Union Maurice Ewing Series*, **3**, 138–153.

Capdevila, R. and Mougenot, D. 1998. Pre-Mesozoic basement of the western Iberian continental margin and its place in the Variscan belt. *In*: Boillot, G., Winterer, E. L. *et al.*. (eds) *Proceedings of the Ocean Drilling Program, Scientific Results, Volume 103*. Ocean Drilling Program, College Station, TX, 3–12.

Carneiro, J.F. and Mesquita, P. 2014. Definition of CCS Provinces with multi-criteria and least cost path analysis. *Energy Procedia*, **63**, 2645–2654, https://doi.org/10.1016/j.egypro.2014.11.287

Carneiro, J.F., Boavida, D. and Silva, R. 2011. First assessment of sources and sinks for carbon capture and geological storage in Portugal. *International Journal of Greenhouse Gas Control*, **5**, 538–548, https://doi.org/10.1016/j.ijggc.2010.08.002

Carneiro, J.F, Martinez, R., Suaréz, I., Zarhloule, Y. and Rimi, A. 2015. Injection rates and cost estimates for CO_2 storage in the west Mediterranean region. *Environmental Earth Sciences*, **73**, 2951–2962, http://doi.org/10.1007/s12665-015-4029-z

Carvalho, J., Matias, H., Torres L., Manupella, G., Pereira, R. and Mendes-Victor, L. 2005. The structural and sedimentary evolution of the Arruda and Lower Tagus sub-basins, Portugal. *Marine and Geology*, **22**, 427–453, http://doi.org/10.1016/j.marpetgeo.2004.11.004

Cavanagh, A., Wilkinson, M. and Haszeldine, S. 2020. *Bridging the Gap, Storage Resource Assessment Methodologies*. EU H2020 STRATEGY CCUS Project 837754.

Chappelier, D. 1992. *Well Logging in Hydrogeology*. A.A. Balkema, Rotterdam, The Netherlands.

CO2CRC 2008. *Storage Capacity Estimation, Site Selection and Characterisation for CO_2 Storage Projects*. CO2CRC Report RPT08-1001. Cooperative Research Centre for Greenhouse Gas Technologies, Canberra.

CSLF 2007. Phase II Final Report from the Task Force for Review and Identification of Standards for CO_2 Storage Capacity Measurement. Task Force on CO_2 Storage Capacity Estimation for the Technical Group (TG) of the Carbon Sequestration Leadership Forum (CSLF).

Cunha, T. 2008. *Gravity Anomalies, Flexure and the Thermo-Mechanical Evolution of the West Iberia Margin and its Conjugate of Newfoundland*. PhD thesis, University of Oxford, Oxford, UK.

DGEG 2020. *Energy-Emission Scenarios up to 2050 Supporting the National Hydrogen Strategy of Portugal*. Directorate-General for Energy and Geology, Division of Research and Renewables, Portugal.

Dias, R. P. 2001. *Neotectónica da Região do Algarve*. PhD thesis, University of Lisbon, Lisbon, Portugal.

Dinis, J. L., Rey, J., Cunha, P. P., Callapez, P. and Pena dos Reis, R. 2008. Stratigraphy and allogenic controls of the western Portugal Cretaceous: an updated synthesis. *Cretaceous Research*, **29**, 772–780, https://doi.org/10.1016/j.cretres.2008.05.027

E-PRTR 2017. European Pollutant Release and Transfer Register (E-PRTR), https://prtr.eea.europa.eu/#/home [accessed 11 March 2019].

EU ETS 2018. European Union Emission Trading System – European Union Transaction Log, https://ec.europa.eu/clima/ets/oha.do [accessed 2 December 2019].

Goodman, A., Hakala, A. *et al.* 2011. U.S. DOE methodology for the development of geologic storage potential for carbon dioxide at the national and regional scale. *International Journal of Greenhouse Gas Control*, **5**, 952–965, https://doi.org/10.1016/j.ijggc.2011.03.010

GPEP 1986. *The Petroleum Potential of Portugal*. Gabinete para a Pesquisa e Exploração de Petróleos (GPEP), Lisbon.

IEA 2017. *Energy Technology Perspectives 2017: Catalysing Energy Technology Transformations*. International Energy Agency (IEA), Paris, https://doi.org/10.1787/energy_tech-2017-en

IEA 2018. Data and Statistics – CO_2 Emissions by Sector in Portugal. International Energy Agency (IEA), Paris, https://www.iea.org/data-and-statistics?country=PORTUGAL&fuel=CO2%20emissions&indicator=CO2BySector

Inverno, C.M.C., Manuppella, G., Zbyszewski, G., Pais, J. and Ribeiro, M.L. 1993. Notícia Explicativa da Folha 42-C Santiago do Cacém. Carta Geológica de Portugal na Escala 1/50 000. Serviços Geológicos de Portugal, Lisbon.

Keys, W.S. 1990. *Borehole Geophysics Applied to Groundwater Investigations*. United States Geological Survey Techniques of Water-Resources Investigations, Book 2, ch. E2.

Kullberg, J.C. 2000. *Evolução tectónica mesozóica da Bacia Lusitaniana*. PhD thesis, University of Lisbon, Lisbon, Portugal.

Leinfelder, R.R. and Wilson, R.C.L. 1998. Third-order sequences in an Upper Jurassic rift-related second-order sequence, central Lusitanian Basin, Portugal. *SEPM Special Publications*, **60**, 507–525.

Lemos de Sousa, M., Correia da Silva, Z.C., Miranda, A. and Rodrigues, C.F. 2007. The COSEQ Pilot Project: CO_2 Sequestration in Douro Coalfield Meta-Anthracites (NW Portugal). Presented at the International Seminar on Perspectives for Near-term CCS Deployment & Capacity Building for Emerging Economies, 17–19 October 2007, Porto Alegre, Brazil.

Lopes, F.C., Cunha, P.P. and Le Gall, B. 2006. Cenozoic seismic stratigraphy and tectonic evolution of the Algarve margin (offshore Portugal, southwestern Iberian Peninsula). *Marine Geology*, **231**, 1–36, https://doi.org/10.1016/j.margeo.2006.05.007

Machado, S., Sampaio, J., Carvalho, J., Dias, R.P., Costa, A. and Oliveira, J.T. 2007. Armazenamento de CO_2 em aquíferos salinos – Hipóteses para Portugal. Presented at A Fossil Fuel on the Road to Sustainability: Conference Cycle 'Energy and Society', 7 November 2007, Lisbon, Portugal.

Marques da Silva, M.A. 1990. *Hidrogeologia del Sistema Multiacuífero Cretácico del Bajo Vouga – Aveiro (Portugal)*. PhD thesis, University of Barcelona, Barcelona, Spain.

Marques da Silva, M.A. 1992. Camadas guia do Cretácico de Aveiro e sua importância hidrogeológica. *Geociências: Revista da Universidade de Aveiro*, **7**, 111–124.

Martinez, R. 2013. *WP4 Final Report*. COMET deliverable 3.4.

Martinez, R., Suárez, I. and Le Nindre, Y.M. 2010. *Site Selection Criteria*. COMET deliverable 3.1.

Masson, D.G., Cartwright, J.A., Pinheiro, L.M., Whitmarsh, R.B. and Beslier, M.O. 1994. Compressional deformation at the ocean–continent transition in the NE Atlantic. *Journal of the Geological Society, London*, **151**, 607–613, https://doi.org/10.1144/gsjgs.151.4.0607

Matias, H. 2007. *Hydrocarbon Potential of the Offshore Algarve Basin*. PhD thesis, University of Lisbon, Lisbon, Portugal.

Mauffret, A., Mougenot, D., Miles, P.R. and Malod, J.A. 1989. Cenozoic deformation and Mesozoic abandoned spreading centre in the Tagus Abyssal Plain (west of Portugal): results of a multichannel seismic survey. *Canadian Journal of Earth Sciences*, **26**, 1101–1123, https://doi.org/10.1139/e89-095

Moita, C., Pronk, E. and Pacheco, J. 1996. *Porto Basin: Seismic Interpretation Report*.

Moita, P., Berrezueta, E. *et al.* 2020. Experiments on mineral carbonation of CO_2 in gabbros from the Sines massif – first results from project InCarbon. *Comunicações Geológicas*, **107**, 91–96.

Murillas, J., Mougenot, D., Boillot, G., Comas, M.C., Banda, E. and Mauffret, A. 1990. Structure and evolution of the Galicia Interior Basin (Atlantic western Iberian continental margin). *Tectonophysics*, **184**, 297–319, https://doi.org/10.1016/0040-1951(90)90445-E

Palin, C. 1976. *Une Série Détritique Terrigène. Les 'Grés de Silves': Trias et Lias Inférieur du Portugal*. Serviços Geológicos de Portugal, Lisbon.

Pereira, R. and Alves, T.M. 2012. Tectono-stratigraphic signature of multiphased rifting on divergent margins (deep-offshore southwest Iberia, North Atlantic). *Tectonics*, **31**, TC4001, https://doi.org/10.1029/2011TC003001

Pereira, N., Carneiro, J.F., Araújo, A., Bezzeghoud, M. and Borges, J. 2014. Seismic and structural geology constraints to the selection of CO_2 storage sites – The case of the onshore Lusitanian basin, Portugal. *Journal of Applied Geophysics*, **102**, 21–38, https://doi.org/10.1016/j.jappgeo.2013.12.001

Pinheiro, L.M., Wilson, R.C.L., Pena dos Reis, R., Whitmarsh, R.B. and Ribeiro, A. 1996. The western Iberia margin: a geophysical and geological overview. *In*: Whitmarsh, R.B., Sawyer, D.S., Klaus, A. and Masson, D.G. (eds) *Proceedings of the Ocean Drilling Program, Scientific Results, Volume 149*. Ocean Drilling Program, College Station, TX, 3–23.

Ramos, A., Fernández, O., Terrinha, P., Muñoz, J.A. and Arnaiz Á, 2020. Paleogeographic evolution of a segmented oblique passive margin: the case of the SW Iberian margin. *International Journal of Earth Sciences,* **109**, 1871–1895, https://doi.org/10.1007/s00531-020-01878-w

Rasmussen, E.S., Lomholt, S., Andersen, C. and Vejbæk, O.V. 1998. Aspects of the structural evolution of the Lusitanian Basin in Portugal and the shelf and slope area offshore Portugal. *Tectonophysics*, **300**, 199–225, https://doi.org/10.1016/S0040-1951(98)00241-8

Ribeiro, A., Antunes, M.T. *et al.* 1979. *Introduction à la Géologie generale du Portugal*. Serviços Geológicos de Portugal, Lisbon.

Ribeiro C. and Terrinha, P. 2007. Formation, deformation and chertification of systematic clastic dykes in a differentially lithified carbonate multilayer. SW Iberia, Algarve Basin, Lower Jurassic. *Sedimentary Geology*, **196**, 201–215, https://doi.org/10.1016/j.sedgeo.2006.06.001

Rocha, R.B. and Soares, A.F. 1984. Algumas reflexões sobre a sedimentação jurássica na orla mesocenozóica ocidental de Portugal. *Memórias e Noticias*, **97**, 133–142.

Romão, I.S., Gando-Ferreira, L.M., da Silva, M.M.V.G. and Zevenhoven, R. 2016. CO_2 sequestration with serpentinite and metaperidotite from Northeast Portugal. *Minerals Engineering*, **94**, 104–114, https://doi.org/10.1016/j.mineng.2016.05.009

Roque, C. 2007. *Tectonostratigrafia do Cenozóico das Margens continentais Sul e Sudoeste portuguesas: um modelo de correlação sismostratigráfica*. PhD thesis, University of Lisbon, Lisbon, Portugal.

Schlumberger 2009. *Log Interpretation Charts*. Schlumberger, Sugar Land, TX.

Seixas, J., Fortes, P. *et al.* 2015. *CO_2 Capture and Storage in Portugal: A Bridge to A Low Carbon Economy*. FCT-UNL, Lisbon.

Taylor, A.M., Gowland, S., Leary S., Keogh K.J. and Martinius, A.W. 2014. Stratigraphical correlation of the Late Jurassic Lourinhã Formation in the Consolação Sub-basin (Lusitanian Basin), Portugal. *Geological Journal*, **49**, 143–162, https://doi.org/10.1002/gj.2505

Terrinha, P. 1998. *Structural Geology and Tectonic Evolution of the Algarve Basin, South Portugal*. PhD thesis, University of London, London, UK.

Terrinha, P., Ribeiro, C., Kullberg, J. C., Lopes, C., Rocha, R. and Ribeiro, A. 2002. Compressive episodes and faunal isolation during rifting, Southwest Iberia. *The Journal of Geology*, **110**, 101–113, https://doi.org/10.1086/324206

Terrinha, P., Pinheiro, L. *et al.* 2003. Tsunamigenic–seismogenic structures, neotectonics, sedimentary processes and slope instability on the southwest Portuguese Margin. *Marine Geology*, **195**, 153-176, https://doi.org/10.1016/S0025-3227(02)00682-5

Terrinha, P., Rocha, R. *et al.* 2006. A Bacia Algarvia: Estratigrafia, paleogeografia e tectónica. *In*: Dias, R., Araújo, A., Terrinha, P. and Kullberg, J.C. (eds) *Geologia de Portugal no Contexto da Ibéria*. University of Évora, Évora, Portugal, 247–316.

Terrinha, P., Kullberg, J.C. *et al.* 2019*a*. Rifting of the Southwest and West Iberia continental margins. *In*: Quesada, C. and Oliveira, J. (eds) *The Geology of Iberia: A Geodynamic Approach*. Regional Geology Reviews. Springer, Cham, Switzerland, 251–283, https://doi.org/10.1007/978-3-030-11295-0_6

Terrinha, P., Ramos, A. *et al.* 2019*b*. The Alpine Orogeny in the West and Southwest Iberia margins. *In*: Quesada, C. and Oliveira, J. (eds) *The Geology of Iberia: A Geodynamic Approach*. Regional Geology Reviews. Springer, Cham, Switzerland, 487–505, https://doi.org/10.1007/978-3-030-11295-0_11

UNFCCC 2015. *Adoption of the Paris Agreement—Proposal by the President; UNFCCC – United Nations Framework Convention on Climate Change: Paris, France, 2015*.

Vangkilde-Pedersen, T., Anthonsen, K.L. *et al.* 2009. Assessing European capacity for geological storage of carbon dioxide – the EU GeoCapacity project. *In*: Gale, J., Herzog, H. and Braitsch, J. (eds) *Proceedings of the 9th International Conference on Greenhouse Gas Control Technologies 2008 (GHGT-9)*. *Energy Procedia*, **1**, 2663–2670.

Wilson, R.C.L. 1988. Mesozoic development of the Lusitanian Basin, Portugal. *Revista de la Sociedad Geológica de Espana*, **1**, 393–407.

Wilson, R.C.L., Hiscott, R.N., Willis, M.G. and Gradstein, F.M. 1989. The Lusitanian basin of west-central Portugal: Mesozoic and Tertiary tectonic, stratigraphy, and subsidence history. *In*: Tankard, A.J. and Balkwill, H.R. (eds) *Extensional tectonics and stratigraphy of the North Atlantic margins,* AAPG Memoir. **40**, 341–361, https://doi.org/10.1306/M46497C22

Winsauer, W.O., Shearin, H.M., Jr, Masson, P.H. and Williams, H. 1952. Resistivity of brine saturated sands in relation to pore geometry. *AAPG Bulletin*, **36**, 253–277.

Witt, W.G. 1977. *Stratigraphy of the Lusitanian Basin*. Shell Prospex Port, Algés, Portugal.

Wyllie, M.R.J., Gregory, A.R. and Gardner, G.H.F. 1958. An experimental investigation of factors affecting elastic wave velocities in porous media. *Geophysics*, **23**, 459–493, https://doi.org/10.1190/1.1438493

Zitellini, N., Chierici, F., Sartori, R. and Torelli, L. 1999. The tectonic source of the 1755 Lisbon earthquake and tsunami. *Annali di Geofisica*, **42**, 49–55.